The conditional ecology of pest suppression: A general mechanistic framework for predicting landscape effects on biological control

Andrew Corbett[1]*, Emily A. Martin[2,3]

[1]Department of Entomology, University of California, Davis, CA

[2]Department of Animal Ecology, Institute of Animal Ecology and Systematics, Justus Liebig University of Gießen, Heinrich-Buff-Ring 26-32, 35392 Gießen, Germany

[3]Liebig Center for Agroecology and Climate Impact Research, Justus Liebig University of Gießen, Germany

*Corresponding author. Email: andcorbett@ucdavis.edu

One-sentence summary

Landscape structure affects pest suppression through two early-season predator mechanisms (immigration and energy accumulation), but pest traits determine how — and whether — these mechanisms translate into reduced pest load, producing three predictable suppression fingerprints.

Abstract

Landscape heterogeneity often increases natural enemy abundance, yet its effects on crop pest suppression are strikingly inconsistent across empirical studies. We developed a trait-based simulation framework to identify the general mechanisms linking landscape structure to realized pest load. Across >150 *in silico* experiments, we show that landscape attributes influence biological control by altering two early-season predator metrics: (i) the immigration rate from the surrounding landscape and (ii) the rate at which colonizing predators accumulate energy after arriving in the crop. These two conditions form universal causal pathways from landscape structure to pest suppression, but their relative importance depends on pest traits. Suppression of slow-growing, diffusely distributed pests requires high early-season energy accumulation by predators; rapidly growing and aggregated pests are controlled by high predator immigration alone; suppression of rapid but diffuse pests requires both, and is weak even under favorable conditions. These three suppression fingerprints explain why landscape heterogeneity reliably increases natural enemy arrival yet only sometimes reduces pest load. Our results reveal a general, trait-mediated architecture—the conditional ecology of pest suppression—that reconciles inconsistent field findings, predicts when landscape heterogeneity should enhance biological control, and provides a mechanistic framework for using landscape management to support sustainable agriculture.

Keywords

Agroecology; Arthropod-plant interactions; Ecological simulation; Ecosystem services; Landscape ecology; Natural pest control; Predator-prey interactions.

1. Introduction

Biological control of insect pests by natural enemies is a cornerstone of sustainable agriculture, yet the ecological processes that govern its effectiveness remain difficult to predict. Across crops and regions, landscape heterogeneity—typically measured as the amount, diversity, or spatial arrangement of non-crop habitat—is widely expected to enhance natural pest suppression by providing refuges and resources for predators (Dainese et al., 2019). Indeed, multiple syntheses report that predator abundance and activity increase with greater heterogeneity (Bianchi et al., 2006; Martin et al., 2019; Priyadarshana et al., 2024). But pest suppression outcomes are far less consistent: in some studies heterogeneity reduces pest pressure, in others it increases it, and in many it has no detectable effect (Dainese et al., 2019; Karp et al., 2018; Poveda et al., 2025; Tamburini et al., 2020). This persistent mismatch between predator responses and pest outcomes limits our ability to design landscapes that reliably support natural pest control.

Why does landscape structure produce such variable suppression outcomes? Several explanations have been proposed, including differences in natural enemy life histories, mismatches in resource timing, natural habitat acting as a refuge for pests as well as enemies, and context-dependent pest dynamics (Begg et al., 2017; Schellhorn et al., 2015; Tscharntke et al., 2016). Empirical studies increasingly recognize that heterogeneity affects predators and pests through multiple mechanisms—dispersal, resource access, overwintering success—but the causal pathways linking these mechanisms to realized pest load remain poorly resolved (Martin et al., 2019). The typical approach, correlating static abundance measures with landscape metrics, cannot capture the dynamic interactions among landscape structure, predator traits, and pest population trajectories. As a result, studies often detect positive effects of heterogeneity on natural enemy abundance without corresponding improvements in pest suppression.

A key limitation of past work is that it treats “predator abundance” as the primary mediator between landscape features and pest suppression. Yet in many biological control systems, especially annual crops, the early season sets the trajectory of pest populations long before peak predator abundance is reached. Preparation for planting clears annual crop fields of many pest insects and natural enemies, requiring colonization from field margins or nearby natural or semi-natural habitat. Upon crop germination, pest insects need simply locate and colonize individual crop plants in order to establish populations. Natural enemies, on the other hand, have the steeper challenge of locating sufficient pest insects to survive and reproduce, or locating supplemental resources such as alternative prey, nectar or pollen. These considerations suggest that two early-season processes should be especially influential: the number of colonizing predators arriving from the surrounding landscape, and the initial energy accumulation, and therefore the longevity, of these colonizers. These processes determine whether predators arrive in the crop in sufficient numbers and subsequently survive, reproduce, and engage prey quickly enough to influence pest trajectories. Crucially, the population growth rate and spatial distribution of the pest insect itself may strongly influence the latter.

Here, we propose that these two early-season predator processes—immigration from overwintering refuges and initial energy accumulation—form universal causal pathways linking landscape structure and in-field resources to pest suppression (Fig. 1). Pest traits are expected to determine which pathway dominates, generating distinct ‘suppression fingerprints’ that resolve previously observed inconsistent effects of landscape heterogeneity on natural pest suppression.

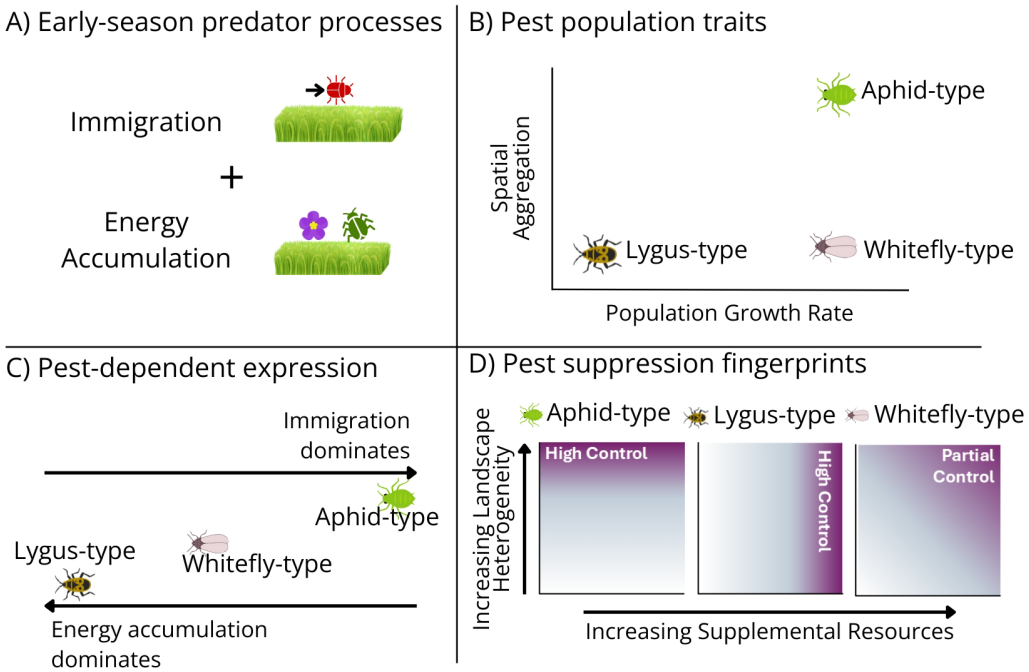

Figure 1. Conceptual framework for the conditional ecology of pest suppression. (A) Landscape structure and in-field resources determine two orthogonal early-season predator processes: immigration and energy accumulation. These processes determine two early-season predator state variables—realized predator abundance in the crop and predator energetic state—which together shape pest suppression. (B) Pest species differ in reproduction rate and spatial aggregation: rapid-growing, aggregated ("aphid-type"); slow-growing, diffuse ("lygus-type"); and rapid-growing, diffuse ("whitefly-type"). (C) Pest traits determine how early-season predator state translates into suppression, with suppression being conditioned by predator abundance (driven by immigration), energy (driven by energy accumulation), or both. (D) The interaction of these axes produces three characteristic pest suppression fingerprints.

Computer simulation has long been used to investigate complex, multiscale systems where controlled experiments are infeasible, such as global climate prediction (Edwards, 2011). To isolate causal pathways across landscape scales that are experimentally inaccessible, we develop a mechanistic simulation framework for biological control in agricultural landscapes that integrates landscape structure, predator dispersal, predator energetics, and pest population dynamics at large spatial scales. Extending previous modeling approaches (Corbett et al., 2024), we simulated a generalist predator that relies on discrete non-crop habitat patches as overwintering refuges and three pest types that differ in growth rate and spatial aggregation—traits that strongly shape predator–prey encounter rates and feedbacks. Across >150 *in silico* experiments, we varied landscape attributes, predator traits, and in-crop resource availability and modelled emergent effects on the resulting pest load at the center of a simulated landscape (Fig. 2).

Our results reveal a simple, generalizable architecture linking landscape structure to pest suppression. Landscape heterogeneity consistently increases early-season predator immigration, but only sometimes decreases pest load. Across pest types, cumulative pest suppression can be understood as a function of the two early-season predator processes of immigration and energy accumulation. These two processes form general causal pathways that link landscape structure

and predator traits to pest suppression. Pest traits determine which pathway matters, producing distinct and predictable signatures in how pest suppression responds to early-season predator processes. These three signatures — suppression fingerprints—resolve long-standing contradictions in empirical landscape studies and explain why predator abundance increases more often than pest suppression.

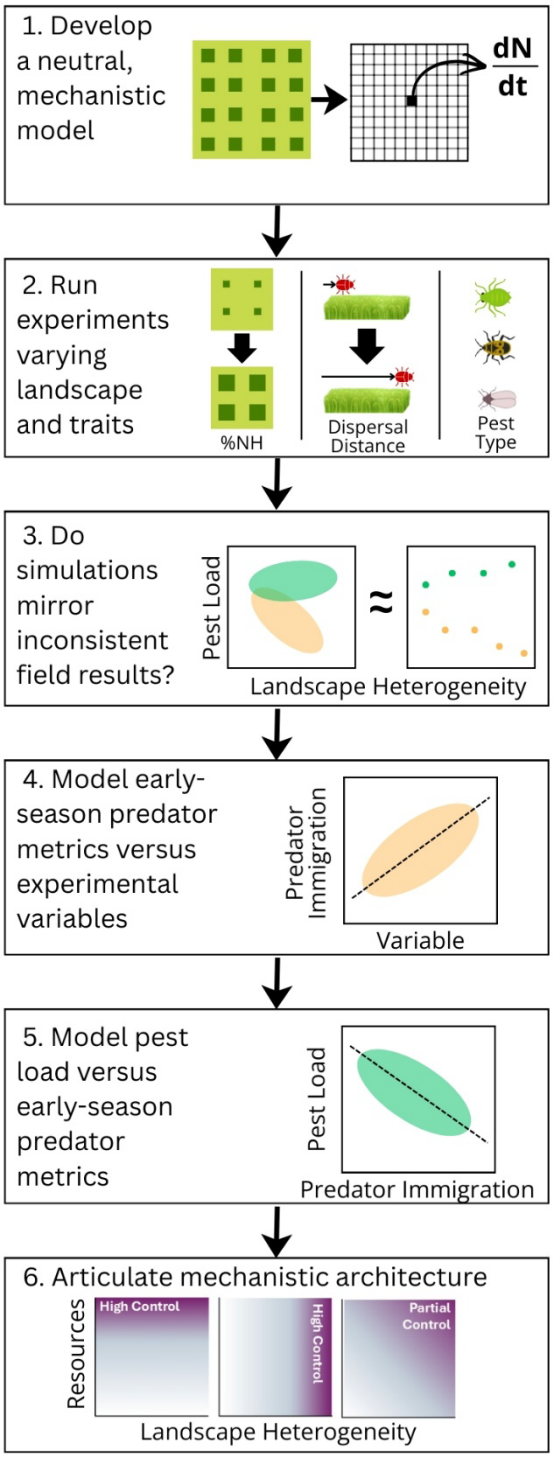

We propose that these fingerprints constitute a general theoretical framework for understanding the conditional ecology of natural pest suppression. By revealing when landscape heterogeneity should and should not enhance biological control, our work provides a mechanistic foundation for designing landscapes that reliably support sustainable agriculture. More broadly, our results show how trait-mediated early-season bottlenecks can generate predictable yet highly variable ecosystem service outcomes across heterogeneous landscapes, thus advancing our understanding of how spatial heterogeneity shapes ecological processes and their outcomes at landscape scales.

Figure 2. Mechanistic analysis pipeline. We first develop (1) a neutral, mechanistic model and (2) use it to generate simulation outcomes across a broad range of landscape and trait combinations. We then (3) assess whether these simulations reproduce the inconsistent patterns observed in field studies, thereby establishing the empirical relevance of the model. From this foundation, we examine how (4) experimental variables shape calculated metrics for the early-season predator processes of immigration and energy accumulation, and (5) evaluate how those metrics influence pest load. Finally, we (6) integrate these components into a coherent mechanistic architecture that explains when increased landscape heterogeneity does, and does not, lead to reduced pest loads in crops.

2. Results

In silico experiments mirror inconsistent responses to landscape structure observed in field studies

Across three contrasting pest types, our *in silico* experiments generated a spectrum of suppression outcomes that mirror the qualitative inconsistencies reported in field studies. For rapid-growing, aggregated pests ("aphid-type"), increasing non-crop habitat (hereafter NH) amount and proximity produced strong and consistent reductions in pest load (Fig. 3A, 3G). For slow-growing, diffusely distributed pests ("lygus-type"), pest load was largely unresponsive to landscape structure but was strongly suppressed by in-crop supplemental resources alone (Fig. 3B, 3H). For rapid-growing but diffuse pests ("whitefly-type"), suppression required both high NH and supplemental resources and rarely exceeded intermediate levels (Fig. 3C, 3I). Effects of NH amount closely tracked predator overwintering density (Fig. 3D,E,F) and NH effects were strongest when NH patches were close to the focal field, consistent with predator dispersal constraints (Fig. 3G,H,I). Collectively, these results show that even with an identical predator system, contrasting pest traits generate three distinct "suppression fingerprints," explaining why empirical landscape effects on pest control are so variable.

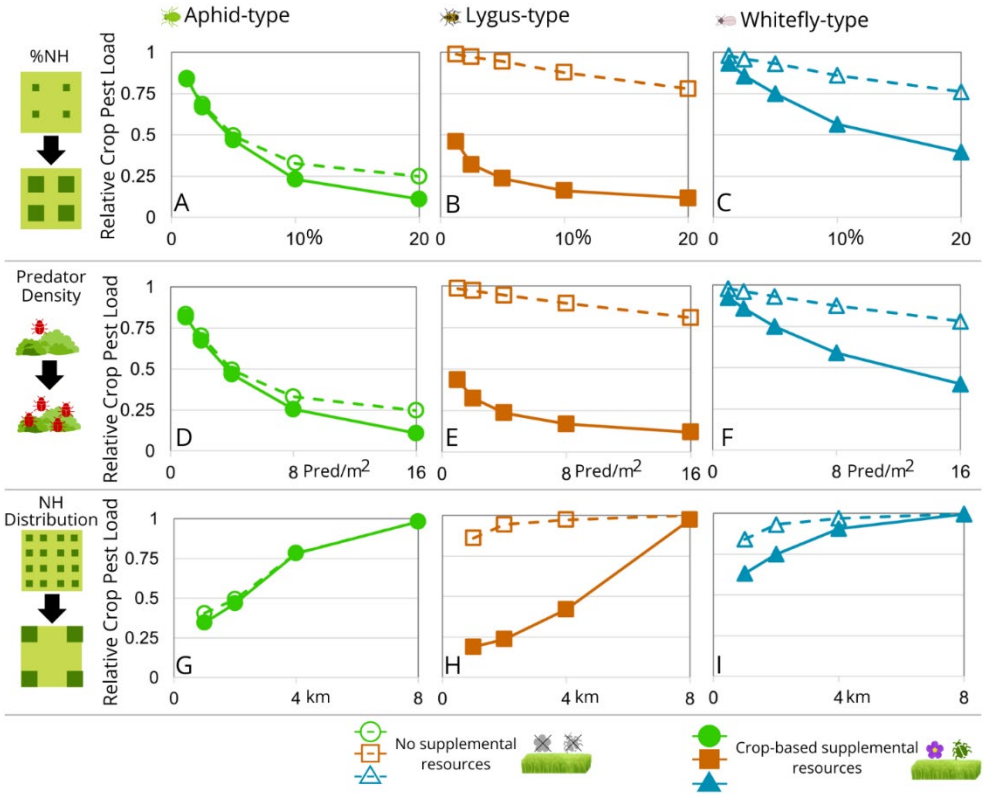

Figure 3. Relative crop pest load vs. landscape attributes – percent non-crop habitat (NH) coverage (A, B, C), predator overwintering density (D, E, F), and distribution of NH patches at varying distances from the focal field (G, H, I) – and for three pest population types – rapid-growing, spatially aggregated ("aphid-type"; A, D, G), slow-growing and diffuse ("lygus-type"; B, E, H), and rapid-growing and diffuse ("whitefly-type"; C, F, I) – with and without crop-based supplemental resources (solid versus dashed lines, respectively). Crop pest load is shown relative to the control simulation without predators for each respective pest population type.

Predator traits moderate natural control outcomes

Although the predator was identical across all simulations, variation in predator traits produced sharply different suppression responses depending on pest type and the presence of supplemental resources (Fig. 4). Synchrony of emergence with the pest and greater likelihood and distance of dispersal each strengthened suppression for aphid-type pests, but had weaker or inconsistent effects for whitefly-type and lygus- type pests. These trait effects were further modulated by crop-based resources, particularly for the lygus-type and whitefly-type pests. Together, these patterns show that predator traits do not act uniformly across systems; instead, their influence depends on how predator behavior interacts with pest traits and resource context. This result motivates the search for early-season processes that translate predator traits into system-specific suppression outcomes, which we address in the next section.

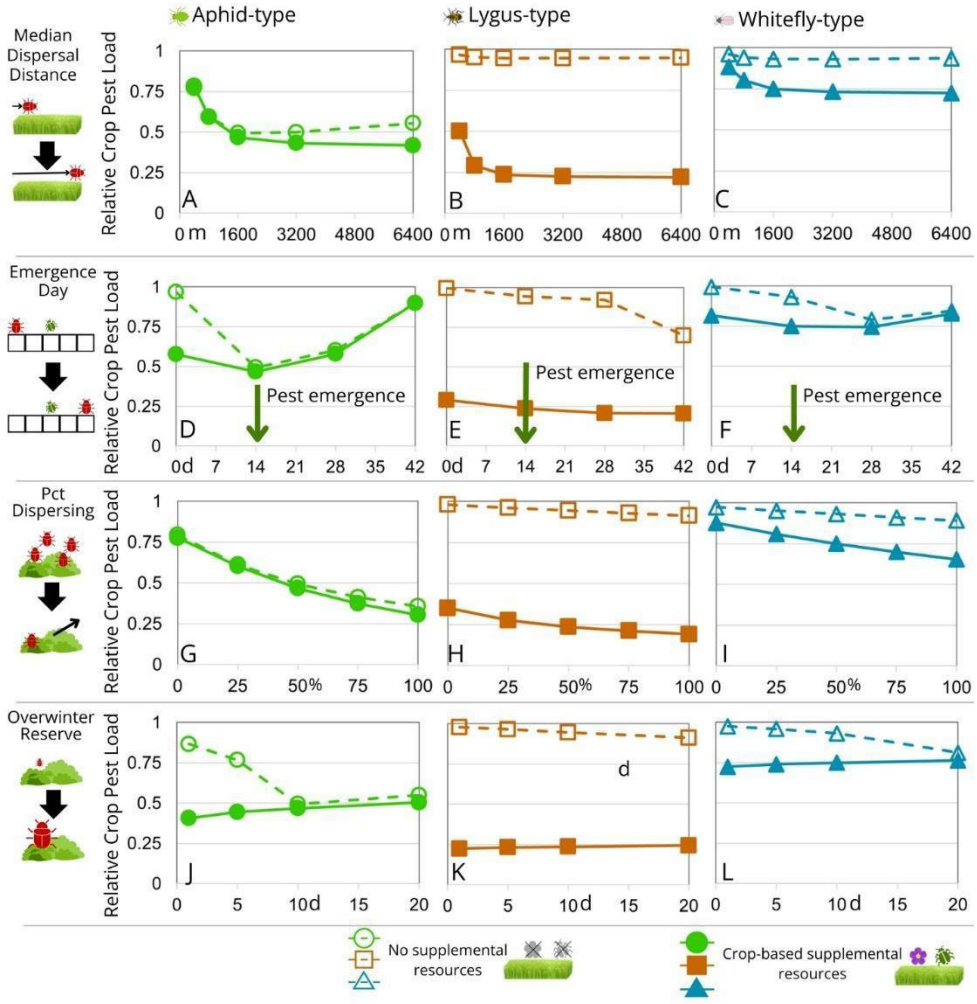

Figure 4. Relative crop pest load vs predator traits – median dispersal distance (A, B, C), day of emergence from overwintering (D, E, F), percent of predators dispersing at emergence (G, H, I), and size of overwintering energy reserve in day's worth of energy (J, K, L) – and for three pest population types – aphid-type (A, D, G, J), lygus-type (B, E, H, K), and whitefly-type (C, F, I, L) – with and without crop-based supplemental resources (solid versus dashed lines, respectively). Crop pest load is shown relative to the control simulation without predators for each respective pest population type.

Experimental variables predict two critical early-season predator metrics

We hypothesized that the apparently inconsistent results of landscape heterogeneity on pest suppression can be understood mechanistically by focusing on two conceptually independent predator processes occurring in the focal field immediately following pest emergence: immigration and energy accumulation. To test this hypothesis we calculated two early-season predator metrics that quantify these key ecological processes:

1. The weekly predator immigration rate during the first 40 days post emergence of the pest;
2. The average per capita energy reserve of predators during the same period.

The first metric measures how many predators colonize the focal field; the second measures access to energy by those colonizers and, in turn, determines their longevity.

We applied linear modeling to each of these two metrics against our experimental variables. We found a distinct separation in which experimental variables predicted which metric (see Supplemental Material for full linear model results). On one hand, predator immigration rate was predicted by predator overwintering density, % NH coverage, NH distribution, the percentage of predators that disperse at emergence, and predators' median dispersal distance. In contrast, per capita energy accumulation by predators was predicted by the presence vs. absence of crop-based supplemental resources, pest population type, predator emergence day, overwintering sugar reserve, and the percentage of predators that disperse at emergence. To quantify the landscape and in-field drivers of these processes, we estimated effect sizes using partial η^2 from the linear models relating our experimental variables and their interaction to predator immigration and per capita early-season energy accumulation. The resulting analyses highlight consistent links between landscape and resource-based factors, and early-season immigration and energy accumulation mechanisms, respectively (Fig. 5):

Landscape and dispersal control of predator immigration

Experimental variables related to landscape structure and predator dispersal behavior explained 82% of variation in predator immigration to the focal field (Fig. 5A). Predator immigration increased strongly with predator overwintering density and percent NH, which were the dominant predictors of predator immigration (partial $\eta^2 = 0.73$ and 0.63, respectively). Increasing NH distribution—bringing patches closer to the focal field—had a secondary positive effect (partial $\eta^2 = 0.24$). Predator dispersal traits modulated these relationships: a higher probability of dispersing at emergence slightly increased immigration to the focal field; higher dispersal distances enhanced immigration only when NH patches lay beyond the predator's median dispersal distance (see for example Fig. 4B). Overall, landscapes with high NH coverage and nearby refuges consistently increased predator arrival into the focal field.

Resource control of early-season predator energy accumulation

Experimental variables related to resource availability in the focal field, or reserves carried by predators into the focal field, accounted for 91% of variability in early-season energy accumulation by predators (Fig. 5B). The presence of crop-based supplemental resources was the dominant variable determining early-season sugar accumulation (partial $\eta^2 = 0.89$). Pest population type was a secondary variable (partial $\eta^2 = 0.56$), with aphid-type pests providing 5.5 additional days' worth of energy than lygus-type pests. The interaction between crop-based supplemental resource availability and pest type also had a dominant influence (partial $\eta^2 = 0.59$): the differences in energy accumulation between pest types were larger in the absence of crop-based supplemental resources. Predator emergence timing played a secondary role in energy accumulation: delayed emergence reduced cumulative energy by shortening the early foraging

window, while earlier emergence limited predator-prey overlap. Initial sugar reserves had weaker effects, enhancing energy accumulation only in the absence of crop-based resources. Finally, predators dispersing immediately upon emergence carried more of those reserves into the focal field than those dispersing later due to local resource scarcity.

Together, these results show that immigration and energy flux are distinct mechanisms, each influenced by separate ecological variables.

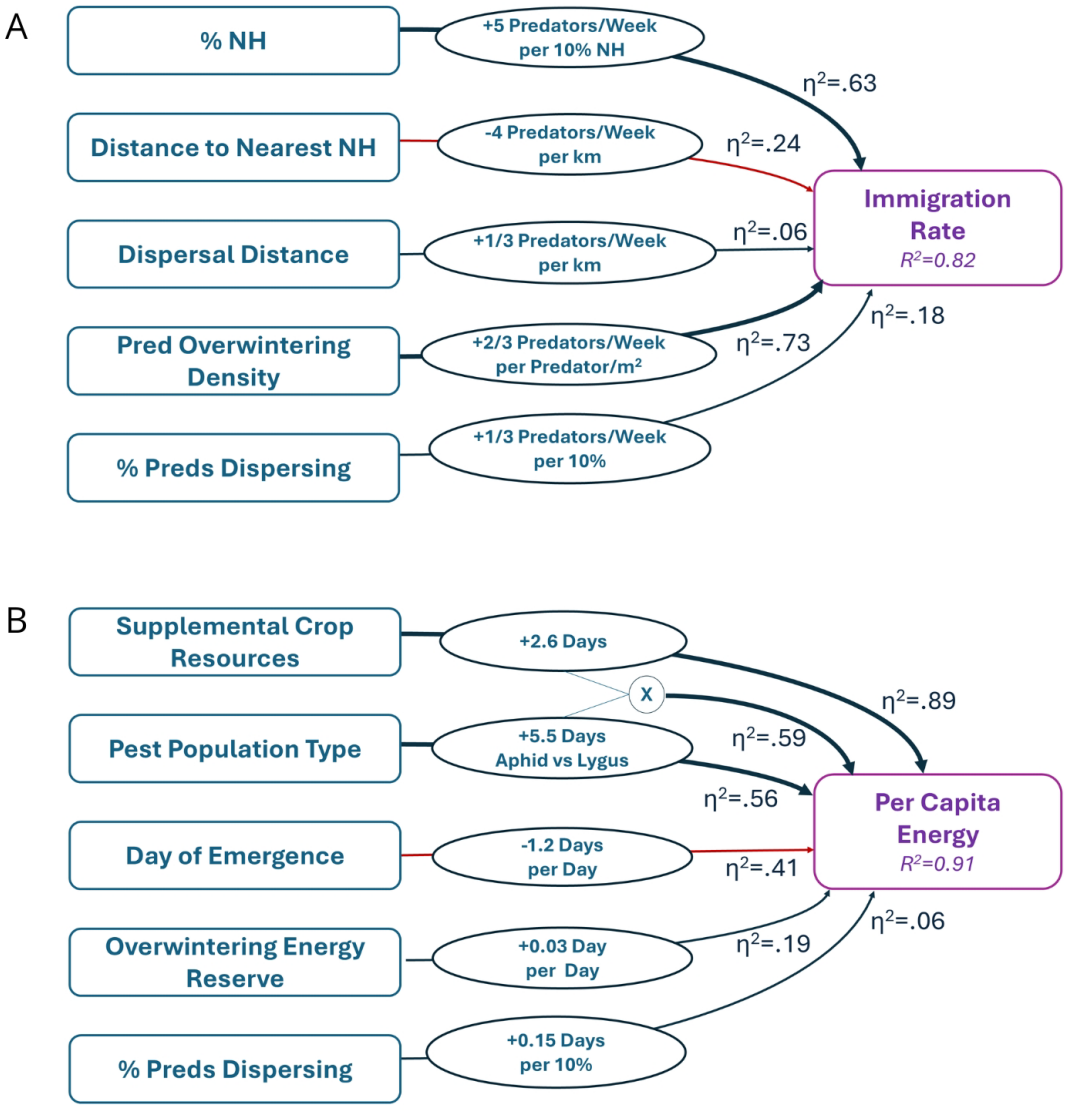

Figure 5. Relative importance (as partial η^2) of experimental variables in explaining variation in immigration rate to the focal field (A) and average per capita energy reserves of predators (B) during the first 40 days following emergence of the pest. Blue arrows indicate positive effects; red arrows indicate negative effects; the weight of arrows is proportional to the size of effect.

Early-season predator metrics predict crop pest load

The two early-season predator metrics — immigration rate and energy accumulation — consistently mediated how landscape attributes translated into pest outcomes (Fig. 6). Differences among pest types reflected the relative dominance of landscape structure (via immigration) versus resource availability (via early-season energy) as the primary driver of suppression. Although landscape structure reliably shaped predator immigration rate, suppression outcomes diverged sharply between pest types depending on how much energy colonizing predators could acquire through early predation. Linear models relating cumulative pest load to immigration and energy accumulation revealed three distinct, predictable "suppression fingerprints" across the three pest population types. Full results of these models are reported in the Supplemental Materials.

Aphid-type pest: immigration-driven fingerprint

For aphid-type pests, suppression increased steeply with predator immigration and showed little sensitivity to early-season energy (Fig. 6A). The linear model confirmed that rapid- growing, aggregated aphid populations were suppressed primarily through predator immigration, with immigration explaining most of the variance in cumulative pest load (partial $\eta^2 = 0.79$) and early-season energy contributing only secondarily (partial $\eta^2 = 0.32$). High immigration generated intense early predation on aggregations, allowing predators to achieve high early-season energy from pest-der ived resources alone. As a result, landscapes with high NH consistently reduced aphid-type pest abundance, even when crop-based resources were absent, lowering cumulative aphid-type load by more than 60% relative to low-immigration scenarios (Fig. 3A).

Lygus-type pest: energy-driven fingerprint

Lygus-type suppression followed an almost entirely different pathway, increasing strongly with early-season energy while remaining largely insensitive to immigration (Fig. 6B). The linear model showed that slow-growi ng, diffusely distributed lygus-type populations were controlled almost entirely through predator energy accumulation, with energy explaining the majority of variation in cumulative pest load (partial $\eta^2 = 0.78$) and immigration having negligible effect. Effective suppression occurred only when predators accumulated substantial early-season energy, typically via crop-based resources. Consequently, suppression was substantial only in landscapes that provided within-field provisioning; landscapes lacking suppl emental resources produced minimal reductions in lygus-type abundance, whereas favorable energy conditions reduced cumulative load by approximately 35–50% (Fig. 3B).

Whitefly-type pest: dual-pathway but weak fingerprint

Whitefly-type pests exhibited a hybr id pattern in which meaningful suppression occurred only when both immigration and early-season energy were high (Fig. 6C). The linear model indicated that rapid-growing but diffuse whitefly -type populations depended on both mechanisms, with immigration and energy each exerting strong effects on cumulative pest load (partial $\eta^2 \geq 0.60$ for both). Predators needed to arrive early and maintain high energetic reserves to exert noticeable control. Even under these favorable conditions, suppression remained modest—typically around

20–30% (Fig. 3C)—reflecting limited predator efficiency when prey reproduce quickly yet are broadly dispersed.

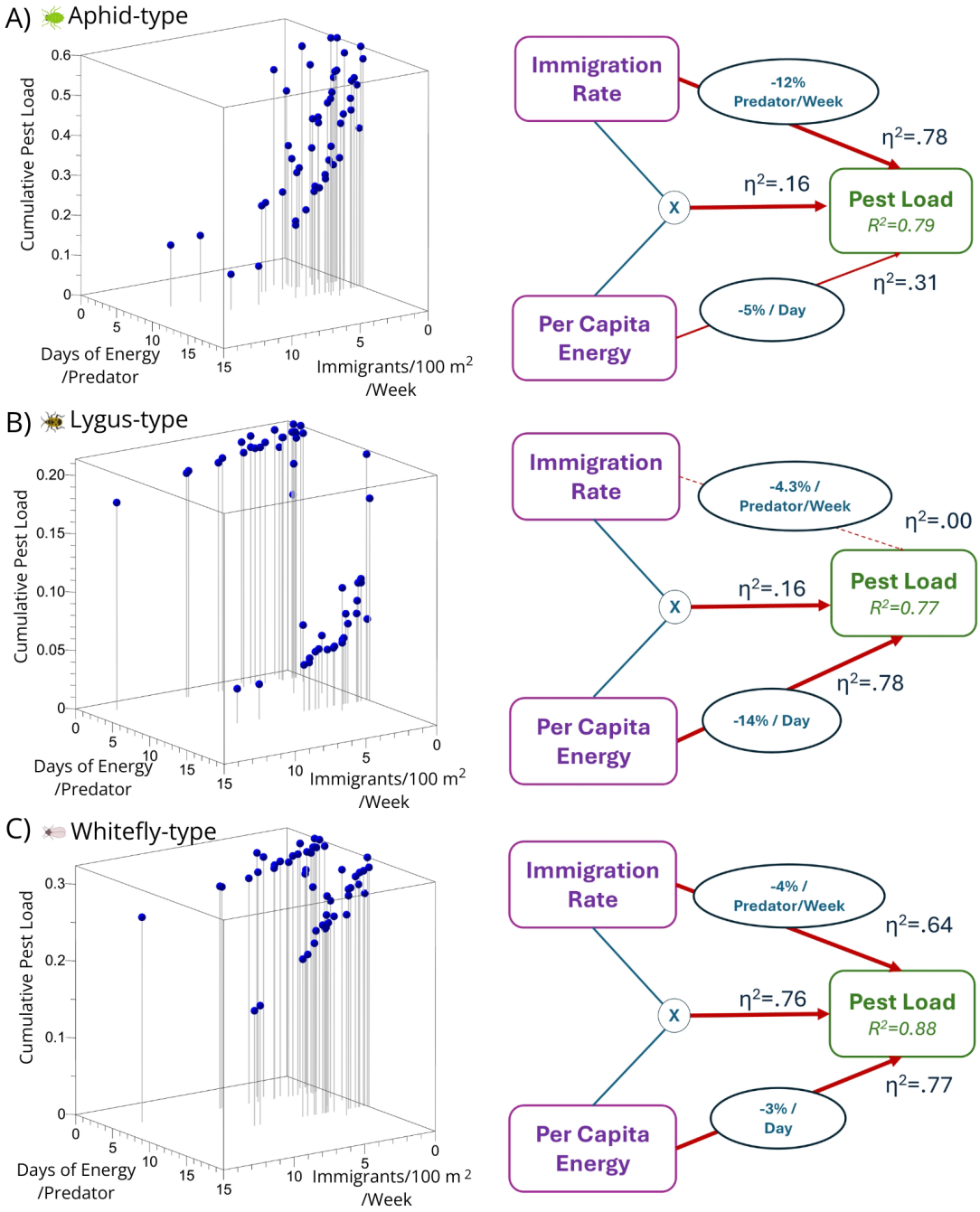

Figure 6. Cumulative pest load of aphid-type (A), lygus-type (B), and whitefly-type (C) pests versus immigration rate and average per capita energy during the first 40 days following pest emergence (left). The right side of figures shows the relative importance (as partial η^2) of predator immigration rate and per capita energy in explaining variation in pest load for the respective pest population type. Blue arrows indicate positive effects; red arrows indicate negative effects; the weight of arrows is proportional to the size of effect.

Why landscape heterogeneity suppresses pests in some systems but not others: A general causal architecture for natural pest suppression

Although NH consistently increased predator immigration, its effect on pest load depended on the alignment of pest traits with early-season processes of immigration and energy acquisition. As a result, landscape heterogeneity led to pest suppression in some systems but not others: biological control of fast-growing and aggregated, aphid-type pests was high whenever landscapes increased immigration. In contrast, biological control of slow-growing and diffuse, lygus-type pests required landscapes that also elevated early-season energy through supplemental resources. Control of fast-growing but diffuse, whitefly-type pests was limited, and was achieved only when both immigration and energy were simultaneously high (Fig. 1D).

Across pest types, these results reveal a consistent causal structure linking landscape attributes to pest outcomes. Landscape structure and predator dispersal traits—including predator overwintering density, NH coverage, distance to NH, dispersal distance, and the proportion dispersing at emergence—determine early- season predator immigration into the focal field. In contrast, resource context (including crop-based supplemental resources, predator emergence timing, initial sugar reserves) and pest population type jointly determine early-season energy accumulation by colonizing predators. Pest population growth rate and degree of aggregation therefore become integral components of the energy axis itself, shaping how much energy predators can acquire early in the season and, in turn, which early-season mechanism — immigration or energy accumulation—dominates suppression in each system.

These relationships produce three general suppression fingerprints for generalist predators across three contrasting pest types and explain why field studies often detect increased predator abundance without consistent pest reductions.

This conditional ecology of pest suppression framework explained 77–88% of variation in cumulative pest load across over 150 landscape × trait × resource combinations. It demonstrates that landscape heterogeneity alone does not drive pest suppression; its effect is mediated by trait-dependent interactions shaping whether increased predator arrival or resource availability translates into reduced pest populations.

3. Discussion

Our simulations reveal that the impact of landscape heterogeneity on biological control is highly contingent on interactions among predator traits, pest population dynamics, and resource availability. While the intuitive expectation—that increasing non-crop habitat (NH) coverage and distribution enhances control—is supported for early-season predator immigration, its translation into reduced pest loads is far from straightforward. Across the three pest types studied, we observed distinct suppression fingerprints, illustrating that landscape heterogeneity alone is insufficient to guarantee effective control.

For the aphid-type pest, suppression is predominantly driven by predator immigration. Rapid prey population growth and spatial aggregation align with predator foraging behavior, ensuring that incoming predators find sufficient resources to establish and reproduce. The fingerprint for this pest type is robust to the absence of crop-based supplemental resources, highlighting a scenario in which landscape heterogeneity directly facilitates biological control. Importantly, our results also

demonstrate sensitivity to predator emergence timing: early arrival risks insufficient prey density for predator establishment, whereas delayed arrival allows the pest population to escape suppression. These mechanistic insights resonate with empirical findings showing that predator arrival timing is critical for aphid suppression (Costamagna et al., 2015). In practice, these results suggest that enhancing NH near fields can reliably reduce aphid-type pressure, provided that natural enemy colonization is synchronized with pest emergence.

The lygus-type pest presents a contrasting scenario. Slow population growth and even spatial distribution render colonizing predators unable to maintain themselves on the pest alone. Here, supplemental crop-based resources—floral resources and alternate prey—become essential for predator persistence and effective pest control. Only under favorable combinations of NH proximity and resource availability does suppression reach high levels, illustrating a strong interaction between landscape structure and within-field conditions. This fingerprint aligns with prior simulations showing that the effectiveness of overwintering refuges is contingent on local resource provisioning (Corbett et al., 2024), and with both field and theoretical studies demonstrating the importance of alternate prey and apparent competition for effective pest suppression (Emery and Mills, 2020; Rosero et al., 2024; Settle et al., 1996). For applied management, this finding underscores the need for integrated habitat and crop-based interventions: simply adding natural habitat outside crops may not suffice to control slow-growing, evenly distributed pests and supplementation with in-field resources may be required.

Whitefly-type pests combine features of both extremes: rapid growth, like aphids, but diffuse distribution, like lygus. Suppression requires both early-season immigration and supplemental resources, yet even under optimal conditions, reductions in pest load are modest relative to the other two types. This fingerprint explains why field studies of whitefly suppression by generalist predators frequently report variable outcomes (e.g., Naranjo et al. 1998). Only landscapes that simultaneously optimize NH coverage, patch proximity, and in-crop resources achieve meaningful control. This highlights the limits of generalized expectations for landscape-mediated biological control and reinforces the importance of trait-based, pest-type-specific understanding.

In line with these mechanistic predictions, empirical studies suggest that aphid–coccinellid systems consistently translate landscape heterogeneity into measurable biological-control responses (Gardiner et al., 2009; Woltz and Landis, 2014), whereas many other pest–predator pairings show increased enemy abundance but inconsistent pest suppression. This contrast is robust across reviews and field studies but is strongly conditioned by pesticide use, refuges, phenology, and spatial scale (Bianchi et al., 2006; Chaplin-Kramer et al., 2011; Rusch et al., 2016; Tscharntke et al., 2005). Across field experiments and syntheses, two consistent patterns emerge. First, aphid control often scales positively with landscape heterogeneity: replicated exclusion and enemy-manipulation experiments, together with syntheses drawing heavily on aphid–coccinellid systems, show that biological control of aphids can increase markedly from simple to complex landscapes, driven by complementary contributions of flying and ground-dwelling enemies and by predator aggregation to aphid patches (Bianchi et al., 2006; Chaplin-Kramer et al., 2011; Rusch et al., 2016). By contrast, studies of other pest–predator pairings (e.g., specialist parasitoid–host systems, non-aggregating pests such as lygus and whitefly with generalist predators, bird-predator systems, or multi-enemy webs) often show scale-dependent or taxon-specific responses: parasitoids and specialist enemies respond at different scales than generalists, and pest suppression is frequently context dependent (Chaplin-Kramer et al., 2011; Gurr et al., 2017; Karp et al., 2018; Letourneau et al., 2009; Martin et al., 2019; Poveda et al., 2025; Rand et al., 2006). Mechanistic reviews and recent models of habitat management and conservation biological control emphasize the same moderators our simulations identified—overwintering/refuge availability, alternate prey, phenology, and spatial scale—as the key factors

determining whether increased enemy abundance translates into effective suppression (Begg et al., 2017; Landis et al., 2000; Rosero et al., 2024; Rusch et al., 2016). In short, our findings help explain both why aphid–coccinellid systems show stronger landscape-driven suppression and why those effects are conditional on management and ecological context.

Our results also provide a mechanistic lens for interpreting pattern-based hypotheses such as the intermediate landscape hypothesis (ILH), which predicts the strongest responses of biodiversity and ecosystem services to management in landscapes of intermediate complexity (Jonsson et al., 2014; Sánchez et al., 2022; Tscharntke et al., 2012). In our simulations, ILH-like behavior emerges most clearly for the whitefly-type pest, where meaningful suppression through increases in in-field resources is contingent on sufficient early-season immigration. More broadly, our framework suggests that whether intermediate landscapes show the strongest management effects depends on the energetic context of colonizing predators, introducing an additional, largely unrecognized axis conditioning ILH patterns. We note that our simulations focus on landscapes ranging from cleared to moderately complex, and extending this framework to highly complex landscapes may further reveal how strong immigration alone could compensate for limiting in-field resources in some systems.

A key insight from our study is the separation between early-season immigration and per capita energy accumulation as drivers of suppression. Across pest types, NH coverage and predator density in refuges consistently drive immigration, while crop-based resources–including both supplemental resources and the pest itself–govern energy accumulation. For aphids, immigration dominates; for lygus, energy accumulation dominates; for whitefly, both interact synergistically. These patterns provide a mechanistic explanation for the mixed empirical results reported in meta-analyses: landscape heterogeneity consistently boosts initial predator abundance, but this only reduces pest loads when pest traits and resource availability align to support establishment of predator populations. Our simulations thus offer a framework for interpreting and predicting variable field outcomes, moving beyond static abundance metrics toward a dynamic, trait-mediated perspective.

The conditional ecology framework emerging from these results has several implications for agroecosystem management. First, identifying the “fingerprint” of a given pest–predator system can inform the design of habitat interventions: managers can tailor NH placement and supplemental resources based on the traits of both pests and natural enemies. Second, understanding the relative importance of immigration versus energy accumulation enables predictions about the temporal window in which interventions are likely to be effective, guiding planting schedules, floral resource provisioning, and timing of natural enemy introductions. Third, by explicitly modeling dispersal distances, our approach highlights spatial constraints on natural control. Landscapes where NH fragments exceed typical dispersal ranges of predators may fail to confer suppression benefits, regardless of overall habitat amount—a consideration often overlooked in field studies.

Beyond applied implications, these findings advance ecological theory. They illustrate how trait-mediated interactions can generate emergent, non-linear outcomes at landscape scales, emphasizing the need for mechanistic, rather than purely correlative, approaches to understanding ecosystem services. Our use of *in silico* experiments allows systematic manipulation of multiple factors—landscape structure, predator traits, pest dynamics—highlighting pathways that would be difficult to disentangle in field studies. The suppression fingerprints we identify suggest that variability in ecological outcomes is not noise, but a predictable consequence of underlying trait and landscape interactions. This insight may extend

beyond agroecosystems to other consumer–resource systems where spatial heterogeneity, dispersal, and resource alignment mediate ecological outcomes.

Several limitations of our study warrant discussion. First, our model assumes a single predator species and three simplified pest types. Real agricultural landscapes contain multiple natural enemies, complex pest assemblages, and additional interactions and behaviours (e.g., hyperpredation, competition, overwintering location) that may modulate outcomes. Second, our simulation represents idealized landscapes with uniform patch shapes and sizes; real landscapes may present more complex configurations that influence dispersal and resource accessibility. Third, we focused on overwintering refuges and in-crop resources, whereas additional ecological drivers—such as non-crop food resources, climatic variation, pesticide use, or interannual shifts in pest phenology—are also likely to shape pest suppression fingerprints. Despite these simplifications, the trait-based framework we propose is generalizable: it can be applied to additional pest–predator systems and extended to explore broader ecological scenarios. Finally, while our simulation results *mirror* the conflicting patterns reported in field studies, we do not claim that our proposed architecture is the only explanation for these empirical inconsistencies; rather, we show that our proposed architecture is *sufficient* to generate a broad spectrum of contradictory outcomes observed in the literature, demonstrating that a single mechanistic structure can account for this diversity. Further field studies and expanded simulation experiments will help test, refine, and extend this mechanistic framework.

In conclusion, our work demonstrates that natural pest suppression is a conditional process governed by interactions among landscape structure, predator traits, and pest dynamics. Landscape heterogeneity alone is not sufficient to guarantee effective control; rather, outcomes depend on the alignment of predator and pest traits with habitat configuration and resource availability. By identifying distinct pest suppression fingerprints, we provide a predictive framework linking landscape ecology to ecosystem service outcomes. These results reconcile apparent contradictions in field studies and offer both theoretical and practical guidance for managing landscapes to enhance natural pest control. The conditional ecology perspective emphasizes that in agroecosystems—as in broader ecological systems—context matters: ecological processes interact in ways that are systematic, interpretable, and ultimately manageable when trait- and landscape-specific mechanisms are considered.

4. Methods

Simulation Framework

We implement a two-dimensional reaction-diffusion model combined with a stochastic dispersal model for adult insects. Each cell contains a classical predator-prey model including age stages for both predator and pest insect and a Type II functional response for the predator. An alternate prey population is also represented in each cell via simple logistic population growth. Crop vegetation is represented as a growing leaf area which achieves its maximum leaf area index (LAI) near mid-season. Predation rate is based on prey density on this growing leaf area. In addition to numbers of adult predators, total energy and egg reserve of adult predators is also represented in each cell. Energy reserves are added to by floral feeding and by prey consumption and deducted based on a daily maintenance cost. Adult predator life span is tied to this energy reserve. Egg reserves are added to by prey consumption and are deducted at a constant rate of oviposition. Adult pests and predators move between cells according to a 2-dimensional diffusion model. Adults also engage in dispersal flights at a rate that is correlated to the current mortality rate in the cell. Dispersal is in a random direction and to random distances; distances are

described by a Weibull probability distribution. Egg and energy reserves move between cells along with adult predators at a per capita rate. Each cell has its own vegetation properties (e.g., maximum LAI and presence/absence of floral resources) and is initialized with its own starting number of overwintering adult predator and prey. The simulated landscape consists of a crop monoculture that is intersected by a grid of field margins (e.g., county road edges) spaced at 1 km intervals, and has patches of NH with varying overall percent coverage and distribution. The pest insect and alternate prey overwinter only in margins; predators overwinter only in NH patches; crops have no resident populations at germination. Full mathematical and implementation details are available in the Supplemental Materials.

Simulation Experiments

We conducted factorial simulations manipulating landscape attributes, pest population dynamics, and predator traits.

Landscape Attributes. We manipulated the following landscape attributes:

1. Percent NH coverage (%NH): Varied from 1.25% to 20% of the landscape tile.
2. NH distribution: Measured as distance from the focal field center to the nearest NH patch, with shorter distances representing higher patch density.
3. Predator overwintering density: Number of predators per m² in NH patches at the start of the simulation.
4. Crop-based supplemental resources: Presence or absence of floral resources and alternate prey within the crop.

Landscape tiles are squares with diagonal length of 16 km (11.3 km × 11.3 km). Patch proximity and distribution were systematically varied to evaluate the interaction between habitat configuration and predator traits.

Pest Population Dynamics. We simulated three pest types reflecting distinct growth and spatial patterns:

1. Aphid-type: Rapid growth, aggregated distribution.
2. Lygus-type: Slow growth, evenly distributed across leaves.
3. Whitefly-type: Rapid growth, diffuse distribution.

Pest life-history parameters, including intrinsic growth rates, dispersal, and aggregation tendencies, were derived from empirical literature and field studies. Pest populations emerged from field margins at the start of the season and grew according to type-specific growth functions.

Predator Traits. Predators were modeled as generalist natural enemies requiring NH patches for overwintering. We manipulated the following traits:

1. Emergence timing: Day of emergence relative to pest appearance, varied across a four-week window.
2. Dispersal distance: Median dispersal distances, ranging from 400 m to 6.4 km.
3. Proportion dispersing at emergence: 0–100% of individuals initiating immediate dispersal.
4. Initial sugar reserve: Energy reserve at emergence, scaled in days of maintenance energy.

Predators consumed pests and supplemental resources according to functional responses, and accumulated energy for reproduction and survival. Predators are assumed to aggregate to prey if prey are aggregated. Early-season energy accumulation was tracked over the first 40 days post-pest emergence.

We calculated metrics for the 1 km^2 crop field at the center of the simulated landscape. The primary response variable was cumulative pest load per cm^2 of leaf surface up to the day of peak population. We also calculated two predator metrics:

1. Predator immigration: Average rate of immigration to the focal field during the first 40 days following pest emergence.
2. Per capita energy accumulation: Average energy reserve per predator over the first 40 days following pest emergence.

We applied linear models to quantify relationships between landscape attributes, predator traits, and focal-field metrics. Partial η^2 was used to estimate effect sizes and rank drivers as dominant (≥0.50), secondary (0.20–0.49), minor (0.05–0.19), or negligible (<0.05). Interaction terms were included to capture synergistic effects between immigration and energy accumulation, as well as between landscape configuration and predator traits. All continuous variables were centered prior to analysis.

Full details on simulation experiments, output processing, and analysis are provided in the Supplemental Materials.

Software

The model was implemented in C++ using the openmp parallel processing library and simulations were run in Windows System for Linux on a desktop computer with a high-end, multi-core CPU. Statistical analyses were conducted in R, using packages lm and lm.beta for linear models and effect size calculations. Figures were generated using Excel for 2D plots and Maple for 3D plots.

5. Data availability

The original code as well as the simulation output used in analyses are available on request from the primary author.

6. Acknowledgements

The authors thank Peter Ellsworth, Daniel Karp, Jay A. Rosenheim and Ricardo Perez-Alvarez for valuable input on early results of this research. This research received no specific grant from any funding agency in the public, commercial, or not-for-profit sectors.

7. Cited references

Begg, G.S., Cook, S.M., Dye, R., Ferrante, M., Franck, P., Lavigne, C., L"ovei, G.L., Mansion-Vaquie, A., Pell, J.K., Petit, S., Quesada, N., 2017. A functional overview of conservation biological control. Crop Protection 97, 145–158.

Bianchi, F.J.J.A., Booij, C.J.H., Tscharntke, T., 2006. Sustainable pest regulation in agricultural landscapes: a review on landscape composition, biodiversity and natural pest control. Proceedings of the Royal Society B 273, 1715–1727.

Chaplin-Kramer, R., O'Rourke, M.E., Blitzer, E.J., Kremen, C., 2011. A meta-analysis of crop pest and natural enemy response to landscape complexity. Ecology Letters 14, 922–932.

Corbett, A., Rosenheim, J., Sivakoff, F., 2024. When can we expect natural habitats to enhance pest control by generalist predators? Insights from a simple, simulated agricultural landscape. Biological Control 191, 105463.

Costamagna, A.C., Venables, W.N., Schellhorn, N.A., 2015. Landscape-Scale Pest Suppression Is Mediated by Timing of Predator Arrival. Ecological Applications 25, 1114–1130. https://doi.org/10.1890/14-1008.1

Dainese, M., Martin, E.A., Aizen, M.A., others, 2019. A global synthesis reveals biodiversity-mediated benefits for crop production. Science Advances 5, eaax0121. https://doi.org/10.1126/sciadv.aax0121

Edwards, P.N., 2011. History of climate modeling. WIREs Climate Change 2, 128–139. https://doi.org/10.1002/wcc.95

Emery, S.E., Mills, N.J., 2020. Effects of predation pressure and prey density on short-term indirect interactions between two prey species that share a common predator. Ecological Entomology 45, 821–830.

Gardiner, M.M., Landis, D.A., Gratton, C., DiFonzo, C.D., O'Neal, M., Chacon, J.M., Wayo, M.T., Schmidt, N.P., Mueller, E.E., Heimpel, G.E., 2009. Landscape diversity enhances biological control of an introduced crop pest in the Midwest USA. Ecological Applications 19, 143–154.

Gurr, G.M., Wratten, S.D., Snyder, W.E., Read, D.M.Y., 2017. Biodiversity and Insect Pests: Key Issues for Sustainable Management. Wiley-Blackwell.

Jonsson, M., Bommarco, R., Ekbom, B., Smith, H.G., Bengtsson, J., Caballero-Lopez, B., Winqvist, C., Olsson, O., 2014. Ecological production functions for biological control services in agricultural landscapes. Methods in Ecology and Evolution 5, 243–252. https://doi.org/10.1111/2041-210X.12149

Karp, D.S., Chaplin-Kramer, R., Meehan, T.D., Martin, E.A., DeClerck, F., Grab, H., Gratton, C., Hunt, L., Larsen, A.E., Martínez-Salinas, A., O'Rourke, M.E., Rusch, A., Poveda, K., Jonsson, M., Rosenheim, J.A., Schellhorn, N.A., Tscharntke, T., Wratten, S.D., Zhang, W., Iverson, A.L., Adler, L.S., Albrecht, M., Alignier, A., Angelella, G.M., Zubair Anjum, M., Avelino, J., Batáry, P., Baveco, J.M., Bianchi, F.J.J.A., Birkhofer, K., Bohnenblust, E.W., Bommarco, R., Brewer, M.J., Caballero-López, B., Carrière, Y., Carvalheiro, L.G., Cayuela, L., Centrella, M., Ćetković, A., Henri, D.C., Chabert, A., Costamagna, A.C., De La Mora, A., De Kraker, J., Desneux, N., Diehl, E., Diekötter, T., Dormann, C.F., Eckberg, J.O., Entling, M.H., Fiedler, D., Franck, P., Frank Van Veen, F.J., Frank, T., Gagic, V., Garratt, M.P.D., Getachew, A., Gonthier, D.J., Goodell, P.B., Graziosi, I., Groves, R.L., Gurr, G.M., Hajian-Forooshani, Z., Heimpel, G.E., Herrmann, J.D., Huseth, A.S., Inclán, D.J., Ingrao, A.J., Iv, P., Jacot, K., Johnson, G.A., Jones, L., Kaiser, M., Kaser, J.M., Keasar, T., Kim, T.N., Kishinevsky, M., Landis, D.A., Lavandero, B., Lavigne, C., Le Ralec, A., Lemessa, D., Letourneau, D.K., Liere, H., Lu, Y., Lubin, Y., Luttermoser, T., Maas, B., Mace, K., Madeira, F., Mader, V., Cortesero, A.M., Marini, L., Martinez, E., Martinson, H.M., Menozzi, P., Mitchell, M.G.E., Miyashita, T., Molina, G.A.R., Molina-Montenegro, M.A., O'Neal, M.E., Opatovsky, I., Ortiz-Martinez, S., Nash, M., Östman, Ö., Ouin, A., Pak, D., Paredes, D., Parsa, S., Parry, H., Perez-Alvarez, R., Perović, D.J., Peterson, J.A., Petit, S., Philpott, S.M., Plantegenest, M., Plećaš, M., Pluess, T., Pons, X., Potts, S.G., Pywell, R.F., Ragsdale, D.W., Rand, T.A., Raymond, L., Ricci, B., Sargent, C., Sarthou, J.-P., Saulais, J., Schäckermann, J., Schmidt, N.P., Schneider, G., Schüepp, C., Sivakoff, F.S., Smith, H.G., Stack Whitney, K., Stutz, S., Szendrei, Z., Takada, M.B., Taki, H., Tamburini, G., Thomson, L.J., Tricault, Y., Tsafack, N., Tschumi, M., Valantin-Morison, M., Van Trinh, M., Van Der Werf, W., Vierling, K.T., Werling, B.P., Wickens, J.B., Wickens, V.J., Woodcock, B.A., Wyckhuys, K., Xiao, H., Yasuda, M., Yoshioka, A., Zou, Y., 2018. Crop pests and predators exhibit inconsistent responses to surrounding landscape composition. Proc. Natl. Acad. Sci. U.S.A. 115. https://doi.org/10.1073/pnas.1800042115

Landis, D.A., Wratten, S.D., Gurr, G.M., 2000. Habitat management to conserve natural enemies of arthropod pests in agriculture. Annual Review of Entomology 45, 175–201.

Letourneau, D.K., Jedlicka, J.A., Bothwell, S.G., Moreno, C.R., 2009. Effects of natural enemy biodiversity on the suppression of arthropod herbivores in terrestrial ecosystems. Annual Review of Ecology, Evolution, and Systematics 40, 573–592.

Martin, E.A., Dainese, M., Clough, Y., Báldi, A., Bommarco, R., Gagic, V., Garratt, M.P.D., Holzschuh, A., Kleijn, D., Kovács-Hostyánszki, A., Marini, L., Potts, S.G., Smith, H.G., Al Hassan, D., Albrecht, M., Andersson, G.K.S., Asís, J.D., Aviron, S., Balzan, M.V., Baños-Picón, L., Bartomeus, I., Batáry, P., Burel, F., Caballero-López, B., Concepción, E.D., Coudrain, V., Dänhardt, J., Diaz, M., Diekötter, T., Dormann, C.F., Duflot, R., Entling, M.H., Farwig, N., Fischer, C., Frank, T., Garibaldi, L.A., Hermann, J., Herzog, F., Inclán, D., Jacot, K., Jauker, F., Jeanneret, P., Kaiser, M., Krauss, J., Le Féon, V., Marshall, J., Moonen, A., Moreno, G., Riedinger, V., Rundlöf, M., Rusch, A., Scheper, J., Schneider, G., Schüepp, C., Stutz, S., Sutter, L., Tamburini, G., Thies, C., Tormos, J., Tscharntke, T., Tschumi, M., Uzman, D., Wagner, C., Zubair-Anjum, M., Steffan-Dewenter, I., 2019. The interplay of landscape composition and configuration: new pathways to manage functional biodiversity and agroecosystem services across Europe. Ecology Letters 22, 1083–1094. https://doi.org/10.1111/ele.13265

Naranjo, S.E., Flint, H.M., Henneberry, T.J., 1998. Effect of insecticides on natural enemies of Bemisia in cotton. Southwestern Entomologist 23, 1–11.

Poveda, K., Karp, D.S., Chaplin-Kramer, R., Centrella, M., Luttermoser, T., Perez-Alvarez, R., O'Rourke, M.E., Martin, E.A., Grab, H., 2025. The Importance of Landscape Composition for Pest Control and Crop Yield: A Global Quantitative Synthesis. Ecology Letters 28, e70250. https://doi.org/10.1111/ele.70250

Priyadarshana, T.S., Martin, E.A., Sirami, C., Woodcock, B.A., Goodale, E., Martínez-Núñez, C., Lee, M., Pagani-Núñez, E., Raderschall, C.A., Brotons, L., Rege, A., Ouin, A., Tscharntke, T., Slade, E.M., 2024. Crop and landscape heterogeneity increase biodiversity in agricultural landscapes: A global review and meta-analysis. Ecology Letters 27, e14412. https://doi.org/10.1111/ele.14412

Rand, T.A., Tylianakis, J.M., Tscharntke, T., 2006. Spillover edge effects: the dispersal of agriculturally subsidized insect natural enemies into adjacent natural habitats. Ecology Letters 9, 603–614. https://doi.org/10.1111/j.1461-0248.2006.00911.x

Rosero, P., Smith, H.G., Pontarp, M., 2024. Impacts of landscape heterogeneity on bottom-up effects affecting biological control. Biological Control 188, 105401.

Rusch, A., Chaplin-Kramer, R., Gardiner, M.M., Hawro, V., Holland, J., Landis, D., Thies, C., Tscharntke, T., Weisser, W.W., Winqvist, C., 2016. Agricultural landscape simplification reduces natural pest control: A quantitative synthesis. Agriculture, Ecosystems & Environment 221, 198–204.

Sánchez, A.C., Jones, S.K., Purvis, A., Estrada-Carmona, N., De Palma, A., 2022. Landscape complexity and functional groups moderate the effect of diversified farming on biodiversity: a global meta-analysis. Agriculture, Ecosystems & Environment 332, 107933.

Schellhorn, N.A., Parry, H.R., Macfadyen, S., Wang, Y., Zalucki, M.P., 2015. Connecting scales: Achieving in-field pest control from areawide and landscape ecology studies. Insect Science 22, 35–51.

Settle, W.H., Ariawan, H., Astuti, E.T., others, 1996. Managing tropical rice pests through conservation of generalist natural enemies and alternative prey. Ecology 77, 1975–1988.

Tamburini, G., Santoiemma, G., E. O'Rourke, M., Bommarco, R., Chaplin-Kramer, R., Dainese, M., Karp, D.S., Kim, T.N., Martin, E.A., Petersen, M., Marini, L., 2020. Species traits elucidate crop pest response to landscape composition: a global analysis. Proc Biol Sci 287, 20202116. https://doi.org/10.1098/rspb.2020.2116

Tscharntke, T., Karp, D.S., Chaplin-Kramer, R., Batáry, P., DeClerck, F., Gratton, C., Hunt, L., Ives, A., Jonsson, M., Larsen, A., 2016. When natural habitat fails to enhance biological pest control–Five hypotheses. Biological Conservation 204, 449–458.

Tscharntke, T., Klein, A.M., Kruess, A., Steffan-Dewenter, I., Thies, C., 2005. Landscape perspectives on agricultural intensification and biodiversity–ecosystem service management. Ecology Letters 8, 857–874.

Tscharntke, T., Tylianakis, J.M., Rand, T.A., Didham, R.K., Fahrig, L., Batáry, P., Bengtsson, J., Clough, Y., Crist, T.O., Dormann, C.F., Ewers, R.M., Fründ, J., Holt, R.D., Holzschuh, A., Klein, A.M., Kleijn, D., Kremen, C., Landis, D.A., Laurance, W., Lindenmayer, D., Scherber, C., Sodhi, N., Steffan-Dewenter, I., Thies, C., Van Der Putten, W.H., Westphal, C., 2012. Landscape moderation of biodiversity patterns and processes - eight hypotheses. Biological Reviews 87, 661–685. https://doi.org/10.1111/j.1469-185X.2011.00216.x

Woltz, M.J., Landis, D.A., 2014. Coccinellid response to landscape composition and configuration. Agricultural and Forest Entomology 16, 341–349.

Supplementary Materials for

The conditional ecology of pest suppression: A general mechanistic framework for predicting landscape effects on biological control

Andrew Corbett and Emily A. Martin

*Corresponding author. Email: andcorbett@ucdavis.edu

This PDF file includes:

Supplementary Text
Figs. S1 to S6
Tables S1 to S11
References (1 to 20)

Supplementary Text

Mathematical Model and Implementation

The model is a reaction-diffusion system for three stages of a pest insect, three stages of a predator, egg and sugar reserves for adult predators, and a single alternate prey stage. Only adult insects undergo diffusion, which represents trivial movement. A dispersal kernel for adult insects is layered on top of this reaction-diffusion model. Egg and sugar reserves move with adult predators diffusing or dispersing on a per capita basis. For clarity and simplicity, we present the local population dynamics as a set of ordinary differential equations. Diffusion and dispersal only applies to adults and are described separately.

Population Dynamics

Pest Population. The pest population is represented by three differential equations for eggs, N_E, juveniles, N_J, and adults N, plus an equation for cumulative pest density, C, plus an equation for overwintering adults, N_O, as follows:

$$(1) \qquad \frac{dN_E}{dt} = b(t)\cdot\frac{N}{2} - ej\cdot N_E - d_i\cdot N_E$$

$$(2) \qquad \frac{dN_J}{dt} = ej\cdot N_E - pN_J\cdot pr(t) - ja\cdot N_J - d_i\cdot N_e$$

$$(3) \qquad \frac{dN_O}{dt} = -emr_{No}(t)\cdot N_O$$

$$(4) \qquad \frac{dN}{dt} = emr_{No}(t)\cdot\left(1 - pDisp_{No}\right)\cdot N_O + ja\cdot N_J - pN\cdot pr(t) - d(t)\cdot N$$

$$(5) \qquad \frac{dC}{dt} = \frac{N + N_J}{L(t)\cdot\theta_L\cdot A}$$

where

$b(t)$ = *Pest oviposition rate at t*

ej = *Egg maturation rate*

d_i = *Mortality rate due to external sources other than predation*

$emr_{No}(t)$ = *Emergence rate of overwintering adults at t*

$pDisp_{No}$ = *Proportion of overwintering adults dispersing at emergence*

pN_J = *Proportion of prey that are juvenile pests*

$pr(t) = Total\ predation\ at\ t$
$ja = Juvenile\ maturation\ rate$
$pN = Proportion\ of\ prey\ that\ are\ adult\ pests$
$d(t) = Adult\ pest\ mortality\ at\ t$
$L(t) = Leaf\ area\ index\ at\ t$
$\theta_L = Proportion\ of\ leaf\ surface\ occupied\ by\ the\ pest\ population\ [degree\ of\ aggregation]$
$A = Total\ ground\ surface\ area\ of\ cell\ (cm^2)$

Oviposition and adult mortality are linear functions of cumulative pest density with fixed maximums and minimums, *C*, given by:

$$b(t) = \begin{cases} b_o, & C < \frac{C_{crit}}{10} \\ b_o + b_s \cdot \left(C - \frac{C_{crit}}{10} \right), & C \geq \frac{C_{crit}}{10} \textbf{ and } C < C_{crit} \\ b_{\min}, & C \geq C_{crit} \end{cases}$$

$$d(t) = \begin{cases} d_o, & C < \frac{C_{crit}}{10} \\ d_o + d_s \cdot \left(C - \frac{C_{crit}}{10} \right), & C \geq \frac{C_{crit}}{10} \textbf{ and } C < C_{crit} \\ d_{\max}, & C \geq C_{crit} \end{cases}$$

where:

$b_o = Intrinsic\ oviposition\ rate\ under\ ideal\ resource\ conditions$
$C_{crit} = Critical\ cumulative\ density$
$b_{\min} = Minimum\ birth\ rate\ under\ poor\ resource\ conditions$
$d_o = Intrisic\ mortality\ rate\ under\ ideal\ resource\ conditions$
$d_{\max} = Maximum\ mortality\ rate\ under\ poor\ resource\ conditions$

$$b_s = \frac{b_{\min} - b_o}{C - \frac{C_{crit}}{10}}$$

$$d_s = \frac{d_{\max} - d_o}{C - \frac{C_{crit}}{10}}$$

Overwintering adult pests emerge at a fixed rate following the day on which emergence commences according to:

$$emr_{No}(t) = \begin{cases} erate_{No} & t > T_{No} \\ 0 & otherwise \end{cases}$$

where:

$erate_{No}$ = *Emergence rate of overwintering adult pests*

T_{No} = *Day of emergence of overwintering adult pests*

Leaf area index is a fixed function of *t* and asymptotically approaches a maximum according to:

$$L(t) = \alpha \cdot \left(1 - e^{-\beta \cdot \left(t + T_{init}\right)}\right)$$

where:

α = *Maximum leaf area index*

β = *Rate of growth of vegetation*

T_{init} = *Days of growth at* $t = 0$

Alternate Prey Population. The alternate prey population grows logistically and has no age structure. It's carrying capacity is based on number per unit leaf surface area. Alternate prey are represent by the differential equations

$$(6) \qquad \frac{dH_O}{dt} = -emr_{Ho}(t) \cdot H_O$$

$$(7) \qquad \frac{dH}{dt} = emr_{Ho}(t) \cdot \left(1 - pDisp_{Ho}\right) \cdot H_O + r \cdot H \cdot \left(1 - \frac{\left(\frac{H}{L(t) \cdot A}\right)}{K_D}\right) - pH \cdot pr(t)$$

where:

$emr_{Ho}(t)$ = *Emergence rate of overwintering alternate prey at t*

$pDisp_{Ho}$ = *Proportion of emerging alternate prey that disperse*

r = *Rate of growth of alternate prey*

K_D = *Carrying capacity of alternate prey in numbers per cm2 leaf surface area*

Overwintering alternate prey emerge at a fixed rate following the day on which emergence commences according to:

$$emr_{Ho}(t) = \begin{cases} erate_{Ho} & t > T_{Ho} \\ 0 & otherwise \end{cases}$$

where:

$erate_{Ho}$ = *Emergence rate of overwintering alternate prey*

T_{Ho} = *Day of emergence of overwintering alternate prey*

Predator Population & Nutrient Reserves. The predator population is represented by three differential equations for eggs, P_E, juveniles, P_J, adults P, and one for overwintering adults, P_O, as follows:

$$(8) \qquad \frac{dP_E}{dt} = o \cdot PC - ej_p \cdot P_E$$

$$(9) \qquad \frac{dP_J}{dt} = ej_p \cdot P_E - ja_P \cdot P_J - d_{pj}(t) \cdot P_J$$

$$(10) \qquad \frac{dP_O}{dt} = -emr_{Po}(t) \cdot P_O$$

$$(11) \qquad \frac{dP}{dt} = emr_{Po}(t) \cdot \left(1 - pDisp_{Po}\right) P_O + ja_P \cdot P_J - d_{pa}(t) \cdot P$$

where:

o = *Rate of conversion of egg reserve to oviposited eggs*
P_C = *Total egg reserve of adult predator population* (*see Eq.* 12)
ej_p = *Maturation rate of eggs* to *juvenile stage*
ja_P = *Maturation rate of juveniles* to *adults*
$d_{pj}(t)$ = *Mortality rate of juveniles*
$emr_{Po}(t)$ = *Emergence rate of overwintering adult predators at t*
$pDisp_{Po}$ = *Proportion of overwintering adult predators that disperse on emergence*
$d_{pa}(t)$ = *Mortality rate of adults*

Additionally, adult predator egg reserves, P_C, and adult predator sugar reserves, P_S, are represented by the differential equations

$$(12) \qquad \frac{dP_C}{dt} = u \cdot pn_c \cdot pr_a(t) \cdot \frac{P}{2} - o \cdot P_C - d_{pa}(t) \cdot P_C$$

$$(13) \qquad \frac{dP_S}{dt} = s_{rsv} \cdot emr_{Po}(t) \cdot \left(1 - pDisp_{Po}\right) \cdot P_O + s_{init} \cdot ja_P \cdot P_J + u \cdot pn_s(t) \cdot pr_a(t) \cdot P + f_s(t) \cdot P - m \cdot P - d_{pa}(t) \cdot P_S$$

where:

u = *The nutritional value of individual prey items*
pn_c = *The proportion of consumed prey going to egg production*
$pr_a(t)$ = *Predation rate by adults at t*
s_{rsv} = *Sugar reserve of emerging overwintering adults*
s_{init} = *Initial sugar reserve of new ecolosed adults*
$pn_s(t)$ = *The proportion of consumed prey going to sugar reserves at t*
$f_s(t)$ = *Rate of floral resource consumption at t*
m = *Daily maintenance costs*

Mortality of juveniles is a function of predation rate and the presence or absence of floral resources and is given by

$$d_{pj}(t) = \begin{cases} pd_{\min} & pr_j(t) \geq pj_{\min} \textbf{ or } flr = \textbf{true} \\ pd_{\max} - pdj_s \cdot pr_j(t) & pr_j(t) < pj_{\min} \textbf{ and } pr_j(t) > 0 \textbf{ and } flr = \textbf{false} \\ pd_{\max} & pr_j(t) = 0 \textbf{ and } flr = \textbf{false} \end{cases}$$

where:

$pd_{\min}$ = *Minimum predator mortality rate*
$pr_j(t)$ = *Predation rate by juveniles*
$pj_{\min}$ = *Minimum predation rate before juvenile mortality starts increasing*
flr = *Boolean : Are floral resources present in this cell? [A static, configured feature of cell]*
$pd_{\max}$ = *Maximum predator mortality rate*

$$pdj_s = \frac{\left(pd_{\max} - pd_{\min}\right)}{pj_{\min}}$$

Mortality of adults is a function of sugar reserves, P_S, and is given by

$$d_{pa}(t) = \begin{cases} pd_{\min} & \frac{P_S}{P} \geq s_{\min} \\ pd_{\max} - pd_s \cdot \frac{P_S}{P} & \frac{P_S}{P} < s_{\min} \textbf{ and } \frac{P_S}{P} > 0 \\ pd_{\max} & \frac{P_S}{P} = 0 \end{cases}$$

where:

$$\frac{P_S}{P} = Per\ capita\ adult\ energy\ reserve$$

$$s_{\min} = Minimum\ per\ capita\ energy\ before\ mortality\ starts\ increasing$$

$$pd_s = \frac{\left(pd_{\max} - pd_{\min}\right)}{s_{\min}}$$

Overwintering adult predators emerge at a fixed rate following the day on which emergence commences according to:

$$emr_{Po}(t) = \begin{cases} erate_{Po} & t > T_{Po} \\ 0 & otherwise \end{cases}$$

where:

$erate_{Po} = Emergence\ rate\ of\ overwintering\ adult\ predators$

$T_{Po} = Day\ of\ emergence\ of\ overwintering\ adult\ predators$

Floral consumption by adult predators is a function of predation rate and the availability of floral resources and is given by

$$f_s(t) = \begin{cases} 0 & flr = \textbf{false or } pr_a(t) \geq pr_{crit} \textbf{ or } \frac{P_S}{P} \geq s_{\max} \\ flr_{\max} \cdot \left(1 - \frac{pr_a(t)}{pr_{crit}}\right) & flr = \textbf{true and } pr_a(t) \leq pr_{crit} \\ flr_{\max} & flr = \textbf{true and } pr_a(t) = 0 \end{cases}$$

where:

$pr_{crit} = Predation\ rate\ at\ which\ predators\ start\ switching\ to\ floral\ resource\ consumption$

$s_{\max} = Maximum\ per\ capita\ sugar\ reserve$

$flr_{\max} = Maximum\ rate\ of\ floral\ resource\ consumption$

Proportion of prey consumption going to the sugar reserve is a step function given by

$$pn_s(t) = \begin{cases} 0 & \frac{P_S}{P} \geq s_{\max} \\ pn_s & otherwise \end{cases}$$

where:

$pn_s = Proportion\ of\ prey\ nutrition\ going\ to\ energy\ reserves$

Predation Rate. Predation by adult predators follows a Type II Holling functional response given by

$$pr_a(t) = \frac{Hol_K \cdot (\delta \cdot \sigma)}{(\delta \cdot \sigma) \cdot Hol_D}$$

where:

$Hol_K = Maximum\ consumption\ rate\ (Holling's\ K\ parameter)$

$\delta = Density\ of\ prey$

$\sigma = Search\ area\ of\ predator$

$Hol_D = Prey\ density\ at\ which\ consumption\ is\ half\ of\ maximum\ (Holling's\ D\ parameter)$

Note that $(\delta \cdot \sigma)$ gives the number of prey available to predators at *t*, where prey density is calculated as

$$\delta = \frac{N + N_J + H}{L(t) \cdot \theta_L \cdot A}$$

where:

$\theta_L = Proportion\ of\ leaf\ surface\ occupied\ by\ the\ pest\ population\ [degree\ of\ aggregation]$

Predation by juvenile predators is a simple proportion, j_{pr}, of predation by adults and is given by

$$pr_j(t) = j_{pr} \cdot pr_a(t)$$

Total predation is then given by

$$pr(t) = pr_a(t) \cdot P + pr_j(t) \cdot P_J$$

which appears in differential equations (2), (4), and (7) in the respective losses to predation terms -- modified by the proportion of total prey represented by that type -- for example,

$$pN_J = \frac{N_J}{N + N_J + H}$$

Diffusion

Adult pest insects, alternate prey, and adult predators engage in trivial movement that is represented via diffusion as

$$(14) \qquad \frac{\partial u}{\partial t} = \nabla \cdot (D(x, y, t) \cdot \nabla u) + R(x, y, t)$$

where:

$u = Adult\ population\ at\ (x, y, t)$

$D(x, y, t) = Diffusion\ coefficient\ at \cdot (x, y, t)\ based\ on\ current\ local\ conditions$

$R(x, y, t) = Reflection\ at\ boundaries\ between\ host\ and\ non-host$

For adult pest insects, diffusion varies with cumulative density, *C* (DEq. 5), according to the equation

$$\mathrm{D}(x,y,t)=\begin{cases}\mathrm{D}_{\min} & C(x,y,t)=0\\ \mathrm{D}_{\min}+\left(\dfrac{\mathrm{D}_{\max}-\mathrm{D}_{\min}}{C_{crit}}\right)\cdot C(x,y,t) & 0\le C(x,y,t)\le C_{crit}\\ \mathrm{D}_{\max} & C(x,y,t)>C_{crit}\end{cases}$$

where:

$\mathrm{D}_{\min}=Minimum\ diffusion\ rate\ of\ adult\ pest\ insects$

$\mathrm{D}_{\max}=Maximum\ diffusion\ rate\ of\ adult\ pest\ insects$

$C(x,y,t)=Cumulative\ pest\ density\ at\cdot(x,y,t)$

For adult predators, diffusion varies with the predation rate $pr_a(t)$, according to the equation

$$\mathrm{D}(x,y,t)=\begin{cases}\mathrm{D}_{\max} & pr_a(x,y,t)=0\\ \mathrm{D}_{\max}+\left(\dfrac{\mathrm{D}_{\min}-\mathrm{D}_{\max}}{Hol_K}\right)\cdot pr_a(x,y,t) & 0\le pr_a(x,y,t)\le Hol_K\\ \mathrm{D}_{\min} & pr_a(x,y,t)>Hol_K\end{cases}$$

where:

$\mathrm{D}_{\max}=Maximum\ diffusion\ rate\ of\ adult\ predators$

$\mathrm{D}_{\min}=Minimum\ diffusion\ rate\ of\ adult\ predators$

$pr_a(x,y,t)=Predation\ rate\ of\ adult\ predators\ at\cdot(x,y,t)$

For alternate prey, the diffusion rate is a constant.

Adult predator egg reserves, P_C (DEq. 12), and sugar reserves, P_S (DEq 13), diffuse along with individual adult predators based on their per capita values. For example, for the egg reserve, if directional flux of adult predators is given by

$$J\left(x,y\to x_d,y_d,t\right)=-\mathrm{D}(x,y,t)\cdot\left(u\left(x_d,y_d,t\right)-u(x,y,t)\right)$$

then

$$\Phi_C\left(x,y\to x_d,y_d,t\right)=\frac{P_C(x,y,t)}{u(x,y,t)}\cdot J\left(x,y\to x_d,y_d,t\right)$$

Where

$D(x, y, t) = Diffusion\ coefficient\ at\ origin$
$u(x, y, t) = Adult\ predators\ at\ origin$
$u(x_d, y_d, t) = Adult\ predators\ at\ destination$
$\Phi_C(x, y \rightarrow x_d, y_d, t) = Flux\ of\ egg\ reserves$

The analogous equation for flux of the sugar reserve, Φ_S, is obtained by substituting P_S for P_C. Adult pest insects and alternate prey undergo proportional reflection at the boundaries between host and non-host vegetation according to the equation

$$R(x, y, t) = \sum_{neighbors(x', y')} D(x, y, t) \cdot u(x, y, t) \cdot \rho \cdot \chi_{host}(x, y) \cdot \left[1 - \chi_{host}(x', y') \right]$$

where:

$\rho = Proportion\ reflected\ back\ at\ boundary\ between\ host\ and\ non-host\ vegetation$
$\chi_{host}(x, y) = Indicator\ function: 1\ if\ host,\ 0\ if\ non-host$

Predators do not reflect at vegetation boundaries.

Dispersal

Adult pest insects, alternate prey, and adult predators engage in long range dispersal at emergence from overwintering and in response to local conditions. The number dispersing from *(x,y)* at *t* is represented by the equation

$$(15) \qquad \Delta(x, y, t) = \varphi(x, y, t) \cdot u(x, y, t) + O(x, y, t)$$

where:

$\Delta(x, y, t) = The\ total\ number\ of\ adults\ dispersing$
$\varphi(x, y, t) = The\ proportion\ dispersing\ in\ response\ to\ current\ local\ conditions$
$u(x, y, t) = Adult\ population\ at\ (x, y, t)$
$O(x, y, t) = The\ number\ of\ emerging\ overwintering\ adults\ dispersing$

For adult pest insects, the dispersal rate is directly proportional to adult mortality, *d(t)* (See DEq 4). So, their dispersal rate is given by

$$\varphi(x, y, t) = \varphi_p \cdot d(t)$$

Likewise, the dispersal rate of adult predators is directly proportional to adult mortality, d_{pa} *(t)* (See DEq 11), and is given by

$$\varphi(x, y, t) = \varphi_p \cdot d_{pa}(t)$$

For alternate prey, dispersal rate is a function of density (See DEq 7) as follows

$$\varphi(x, y, t) = \begin{cases} \varphi_p & \dfrac{\left(\dfrac{H}{L(t) \cdot A}\right)}{K_{\mathrm{D}}} > 0.5 \\ 0 & otherwise \end{cases}$$

In each of the above equations for $\varphi(x, y, t)$,

$$\varphi_p \in \left(\varphi_{pest}, \varphi_{pred}, \varphi_{alt-prey}\right), \textit{depending on the population}$$

For pest insects, $\mathrm{O}(x, y, t)$, is calculated as follows (See DEq 3)

$$\mathrm{O}(x, y, t) = emr_{No}(t) \cdot N_{\mathrm{O}} \cdot pDisp_{No}$$

and is calculated in like manner with the analogous parameters for emerging predators (See DEq 6) and emerging alternate prey (See DEq 10).

Assignment of dispersers to new locations in the landscape is handled stochastically as whole numbers. First, the integer number dispersing is obtained via stochastic rounding by

$$\Delta_{actual}(x, y, t) = \begin{cases} \mathrm{floor}\left(\Delta(x, y, t)\right) + 1 & U < \mathrm{frac}\left(\Delta(x, y, t)\right) \\ \mathrm{floor}\left(\Delta(x, y, t)\right) & otherwise \end{cases}$$

where:

$U = A\ uniform\ random\ variate\ on\ U(0, 1)$

$\mathrm{floor}\left(\Delta(x, y, t)\right) = Whole\ number\ part\ of\ \Delta(x, y, t)$

$\mathrm{frac}\left(\Delta(x, y, t)\right) = The\ fractional\ part\ of\ \Delta(x, y, t)$

For each individual disperser, a flight distance is randomly drawn from a Weibull distribution given by the function

$$W_{\mathrm{D}}(d) = \frac{k}{\lambda} \cdot \left(\frac{d}{\lambda}\right)^{k-1} \cdot \mathrm{e}^{-\left(\left(\frac{d}{\lambda}\right)\right)^{k}}$$

where:

$k = Shape\ parameter,\ determining\ shape\ of\ the\ distribution$

$\lambda = Scale\ paramter,\ determining\ median\ flight\ distance$

A flight direction for each disperser is obtained by

$$v = 360 \cdot U$$

The destination (x_d, y_d) is then obtained from $W_{\mathrm{D}}(d)$ and *v* via trigonometry relative to *(x,y)* using the sampled flight distance and direction.

The flux of predator egg reserves is given in similar manner as for diffusion by

$$\Phi_C\left(x, y \to x_d, y_d, t\right) = \frac{P_C(x, y, t)}{u(x, y, t)} \cdot \Delta_{actual}\left(x, y \to x_d, y_d, t\right)$$

where

$$P_C(x, y, t) = Adult\,predator\,sugar\,reserves \quad [DEq\ 12]$$

$$\Delta_{actual}\left(x, y \to x_d, y_d, t\right) = Flux\,of\,adult\,predators\,from\,origin\,to\ \left(x_d, y_d\right)\ via\,dispersal$$

with flow of the sugar reserve, Φ_S, being obtained by substituting P_S for P_C.

Implementation

The above model is numerically solved for a grid of 1130 x 1130 cells, each 10 x 10 m, representing a square landscape tile 16km on the diagonal. Each cell advances its own system of differential equations as described under Population Dynamics via the Euler method. Diffusion of adults is solved using a forward-difference scheme. Dispersal is calculated at each time step after the within cell system has been advanced and adults have been redistributed via diffusion. A time step of 0.05 is used for both within cell and diffusion updates.

The model was implemented in C++ on Windows System for Linux using the Linux g++ compiler. We employed the openmp library (http://www.openmp.org) to enable parallel processing – calculations for individual cells were distributed to multiple processors whenever there was no dependence between cells. Stochastic algorithms were implemented using a Mersenne Twister random number generator seeded via a call to the C++ library function random_device as implemented for the Windows System for Linux. All scenarios were run on a AMD Ryzen 9 7850X processor.

The C++ implementation was validated by ensuring it met the following criteria:

1. Output of the within-cell model implemented in C++ closely approximates that generated by the same system of differential equations implemented in Maple 2021.
2. When adults and energy reserves originate from a point source (large values in a single cell, zero elsewhere), diffusion calculations generate distributions over time that closely approximate a normal distribution with a standard deviation of 2Dt.
3. Adults and energy reserves diffuse independently. I.e., if an area with low numbers of adults but high energy reserves is next to an area with high numbers of adults but low energy reserves, the net movement of adults and energy are in opposite directions.
4. Simulated flight distances closely approximate the corresponding Weibull distribution.

Parameterization

Tables S1-S4 list all parameters used in the model with explanations and references where applicable. Rationale for selected parameters are explained below.

Rationale for parameter value for the energy consumed per day by a predatory bug feeding on floral resources.

We perform a crude calculation, based on various information available in the literature, to provide a realistic starting point for estimating the amount of energy consumed per day by a predatory bug feeding on floral resources. Our approach is as follows:

1) Find an experimentally measured rate of floral energy consumption:
   May (S1) estimates that *Agraulis*, a nectarivorous butterfly, consumes 0.6 J of energy per second via floral feeding.
2) Scale that value based on the mass of *Geocoris* relative to *Agraulis:*
   Cardoso & Gilbert (S2) calculate a dry weight of 50 mg for *Agraulis*. Cohen & Staten (S3) calculate a dry weight of 1.8 mg for *Geocoris*. This yields an estimate for energy consumed by *Geocoris* per minute of
   (0.6 J/s) x (1.8 mg/50 mg) x 60 s = 1.3 J/m
3) Determine how many days of maintenance this represents for *Geocoris*:
   Cohen & Byrne (S4) estimates a daily expenditure for maintenance of 3.6 J for *Geocoris*. This yields an estimate for days-of-maintenance consumed per minute by Geocoris of
   1.3 J/3.6 J = 0.36 days/minute
   Which is equal to roughly 21 days of maintenance every hour, or 518 days per day.

We divide this value by 10, yielding our parameter of value 50 days of maintenance energy consumed per day by a predatory bug feeding on floral resources. Our reasoning is as follows: (a) There will be a search and handling time associated with consumption of floral resources, decreasing the actual amount of energy they can consume per unit time; (b) floral resources are a supplementary resource for *Geocoris* and they are likely much less efficient than *Agraulis* at feeding on floral resources; and, (c) we have not accounted for allometric effects, therefore the actual consumption rate by *Geocoris* is likely to be less than that estimated via a simple linear scaling. Since we assume a maximum energy reserve of 10 days'-worth of maintenance energy, our generalist predator obtains this maximum reserve in roughly 5 hours of feeding exclusively on floral resources. We consider this to be a generous estimate of the potential value of floral resources to a predatory bug.

Rationale for the parameter value for overwintering densities of pest insects and predators.

We generated rough estimates of overwintering density of *Lygus, Geocoris, Orius* in non-crop vegetation from two different sources as follows:

1) Horton & Lewis (S5) estimate the average number of overwintering *Lygus, Geocoris*, and *Orius* per 5 common mullein plants at 10, 15, and 0.6 respectively. Data presented Reinartz (S6) estimates the density of a stand of mullein at up to 5 plants per m^2. Therefore, the per-5-plants estimates by Horton & Lewis (S5) is also a rough estimate for m^2 density.

2) Fye (S7) estimated late-summer density in pigweed – which we take as a rough equivalent to overwintering density – to be 1.2, 1.1, and 2.1 per m2 for *Lygus, Geocoris*, and *Orius* respectively.

We use overwintering densities that are at the higher end of these two estimates.

Rationale for Weibull distribution parameters

The Weibull function defines a family of probability distributions and is expressed as

$$\frac{k}{\lambda}\left(\frac{x}{\lambda}\right)^{k-1} e^{-\left(\frac{x}{\lambda}\right)^{k}}$$

where *k* is the shape parameter and λ is the distance (or scale) parameter. Different values of the shape parameter determine the shape of the distribution; for example, a negative exponential distribution, a normal distribution, or a fat-tail distribution. The distance parameter determines the central tendency of the distribution.

Sivakoff et al. (S8) reports a field study in which insects in a field of alfalfa were sprayed with animal-based proteins, the field was subsequently cut, and insects collected in adjacent cotton were analyzed via ELISA to identify those that originated in the alfalfa field. We used data from this study to choose the value of the Weibull shape parameter as follows:

1. We adapted the simulation model presented in this paper to simulate only diffusion and dispersal by the pest insect and predator without any mortality or reproduction.
2. We used the mean squared displacements reported in Sivakoff et al. (S8) to calculate a distance parameter of 1600.
3. We ran the adapted simulation for multiple values of the shape parameter, *k*, using this distance parameter value (λ=1600). The distribution of adults at day 5 was taken as the model's prediction of the expected distribution of individuals under the respective Weibull parameters. The simulated distributions are shown in Fig. S1, together with the actual distribution of *Lygus* and *Geocoris*.
4. A visual examination suggests that the recaptures for both *Lygus* and *Geocoris* are consistent with a shape parameter value of k=1.5. A Goodness-of-fit test comparing simulated distributions to the recapture distributions (averaged across the 5 days) supports this conclusion. Simulated transects for values other than 1.5 were a poor fit to the recapture data, all of them having $p<0.001$ of being from the same distribution; for a value of k=1.5, $p>0.25$ that simulated and actual recaptures were from the same distribution.

Accordingly, for our simulation study we use shape parameter of k=1.5 for both the generalist predator and the pest insect and a distance parameter in our simulations, λ=1600.

In silico experiments

Landscape structure

Experiments are conducted on a square landscape tile that is 11.3 km on a side – this is equivalent to a diagonal length of approximately 16 km. Boundary conditions are reflective to movement: diffusion uses reflective (mirror) boundaries, whereas long-distance dispersal uses toroidal wrap-around. Because the landscape structure is symmetric and the focal field is centered, these two boundary behaviors produce effectively equivalent edge dynamics. As a result, the simulation predicts the dynamics that occur on a hypothetical "infinite" landscape composed of repeating tiles of the same size and structure. Spatial resolution is 10 × 10 meters, so the grid dimensions are 1130 × 1130 cells.

Each cell has one of three possible vegetation types: crop, natural habitat (NH), or uncultivated margins. By default, all cells represent crop vegetation; thus, the landscape is a pure crop monoculture interrupted by margins and NH patches. Uncultivated margins occur on the landscape grid every 100 rows and every 100 columns, beginning at row and column 50; thus, they are 1km apart and 10 m wide. The pest insect and alternate prey overwinter as adults in these margins, which can be thought of as "county roads" crisscrossing the agricultural landscape; the generalist predator only overwinters in NH patches.

For ease of implementation, whether a cell is crop or NH is specified at the resolution of hectares, which corresponds to a grid of 113 x 113 hectares. The configuration of NH in the landscape varies between experiments based on (1) the percentage of the landscape occupied by NH and (2) the distribution of NH across the landscape. NH is always evenly distributed across the landscape but is broken into different numbers of patches for different experiments. The generalist predator overwinters in and disperses from these NH patches at the beginning of the simulated season. A simple CSV file containing a matrix of 113 x 113 codes specifies the configuration of NH patches in the landscape for any single experiment. Further details are provided below under *Landscape variables*.

Pest types

We define three pest population types based on population growth rate and spatial aggregation (see Table S5):

- The lygus-type pest has slow population growth relative to the predator and is evenly dispersed across the crop leaf surface (e.g., *Lygus* spp. on California cotton).
- The whitefly-type pest exhibits rapid population growth but remains evenly dispersed (e.g., *Bemisia tabaci* on California tomato).
- The aphid-type pest exhibits rapid population growth and strong spatial aggregation (e.g., aphids in Midwest US corn systems). For the aphid-type, we simulate predator aggregation by restricting interaction to a fixed proportion of crop leaf surface area, reflecting localized foraging in prey-dense canopy zones. This operationalizes spatial concentration without requiring explicit spatial modeling.

Pest population types also vary in the peak density achieved. For comparative purposes, Table S5 shows the peak number of nymphs and adults present on a 100 cm^2 leaf. These peak numbers approximate the treatment thresholds for aphids, Lygus, and whitefly in cotton in California. Since pest populations in the field can greatly exceed these thresholds, we performed a sensitivity test to ensure that our key results were unaffected by large increases in simulated pest density which is described below.

All simulation experiments defined below were conducted separately for each of these pest population types by configuring the pest parameter values according to Table S5.

Controls

For comparison of the effects of parameter variation *within* pest population types, we require a simulation to use as a control. For this we use a landscape consisting of the crop with uncultivated margins as described above, but with no NH patches and therefore no generalist predator. We ran this control simulation for each pest population type giving us the crop pest load achieved by that pest type in the absence of any predation; all other simulation experiments include predators.

Experimental variables

We used a bracketing design to evaluate the effects of landscape and predator parameters. We used this approach because a full factorial across all landscape and predator parameters would be computationally prohibitive and unnecessary for isolating the causal influence of each parameter on predator dynamics and pest load. Baseline conditions were defined as 5% NH coverage distributed across 16 patches, no supplemental resources in the crop, and baseline values for all predator traits (Table S6). Each experiment varied a single landscape or predator parameter above or below its baseline value. All bracketing experiments were then run for each pest type both with alternate prey and floral resources available in the crop and without; the response variable is cumulative pest density, expressed relative to the control for that pest type. This resulted in 52 simulation experiments plus one control (see above) for each pest population type, for a total of 159 simulations. See Table S6 for the full list of parameter values used for landscape attributes and predator traits.

Figure S2 shows the distribution of NH patches for the four different landscape configurations of natural habitat listed in Table 2 at 5% total NH coverage. Because crop and NH vegetation are specified at a one-hectare resolution (see Landscape structure, above), patch sizes in a given experiment are not always perfectly uniform in area or shape; the number of hectares required to achieve the desired percent NH coverage does not always divide evenly among the specified number of patches. However, the resulting variation among patches is small and does not affect interpretation. The exact landscape configurations used can be found in the configuration files provided with the code repository.

Figures S3-S5 show population trends in the central focal-field for the pest insect, alternate prey, and predator under baseline conditions for all three pest population types.

Analysis of output

Simulation output

The simulation writes key state variables and metrics for individual cells to an output file every 5 days and for every fifth row and column of cells. For our analysis we use the following output variables:

- Cumulative prey per cm^2 leaf area up to time t
- Number of predators immigrating to the cell during the Δt immediately preceding time t
- Energy units per predator at time t

We are interested in the effects of our experimental variables on pest load and predator dynamics in the $1km^2$ focal field at the center of the landscape tile, outlined in red on the illustrations in Fig. S2. This follows standard practice in landscape ecology: using a focal field preserves the effects of landscape gradients such as distance to the nearest NH patch, which would be obscured if metrics were averaged across the entire landscape. The focal filed corresponds to rows and columns 515 to 615 in our 1130 x 1130 grid. With every fifth cell (by row and column) being sampled, this results in 400 sample points across the focal field every 5 days.

Cumulative pest load

Cumulative pest density is a state variable in our model given by Eq. 5 under Mathematical Model; it captures the total pest pressure experienced by the crop up to time t. Because the three pest types followed different population trajectories in the control simulations—reaching their peaks at different times and at different densities—we standardized comparisons by measuring cumulative pest density up to the peak day in the control simulation for each pest type. Using the control peak day as a fixed reference ensures that cumulative pest load is measured over a consistent developmental window across all experiments for each pest type. These peak days were day 60, day 120, and day 75 for the aphid-, lygus-, and whitefly-type pests, respectively.

Analyses and plots of crop pest load versus predator metrics (Figs. 5 and 6 in main text) use average cumulative pest density to peak population day in the focal field. Plots of the effects of experimental variables (Figs. 3 and 4 in main text) use relative pest load calculated as the average cumulative pest load to peak day in a simulation experiment (See Table S5) divided by the average cumulative pest load to peak day in the control simulation for that pest type.

Predator metrics

Our objective is to measure the status of the predator population early in the season—the period over which predator colonization and subsequent population growth determine their influence on later pest dynamics. Although the exact length of the early-season

window is not biologically fixed, inspection of population trajectories across many simulations showed that predators consistently colonize and either establish or fail to establish within the first 40 days after pest emergence. We therefore use this 40-day period (days 15–55) as the ecologically relevant window for quantifying early-season predator status. Although this window represents different proportions of the time to peak between pest types (see above), this asymmetry reflects real differences in pest population trajectories during this early-season window and is essential for interpreting their effects on natural control.

Immigration. We calculate the average number of predators immigrating to cells in the focal field across the 400 sample cells and the 8 sampling days (see *Simulation output*) spanning days 15 to 55. Since the simulation output is in numbers immigrating over the preceding time step, and $\Delta t = 0.05$, our metric becomes the average sampled immigration divided by 0.4 (8 x 0.05). Our metric then becomes a measure of the early-season immigration rate to the focal field – that is, the average number of predators immigrating per cell per day during the 40-day early-season window. Because immigration counts include arrivals from both outside and within the focal field, this metric may slightly overestimate true external colonization. However, examination of immigration and emigration events indicates that emigration from the focal field is rare, even when median dispersal distance is low, so any inflation is minor and does not materially affect interpretation.

Energy accumulation. For the energy accumulation metric, we calculate the average per capita energy content of predators in the focal field across the 400 sample cells and the 8 sampling days (see *Simulation output*) spanning days 15 to 55.

Table S7 shows full linear model results for predator immigration versus experimental variables; Table S8 shows linear model results for energy accumulation versus experimental variables. Tables S9 through S11 show linear model results for pest load versus predator metrics for aphid-type, lygus-type, and whitefly-type pests, respectively.

Test of sensitivity to peak pest populations

To evaluate the sensitivity of our primary results and conclusions to peak pest density, we ran simulation experiments at increased critical density of our three pest population types for baseline configurations: 1.0 vs 0.5 for aphid-type, 0.4 vs 0.25 for lygus-type, and 0.6 vs 0.3 for whitefly-type. Simulations were run at baseline parameter values and default landscape configurations. The aphid-type pest reached a peak density of 12.0/leaf (assuming 100 cm^2 per leaf) in the absence of predators, the lygus-type pest reached a peak density of 1.6/leaf, and the whitefly-type reached 5.3/leaf. These were each 2 times the peak pest densities in our main experiments (See Table S5).

The relative effect of predator overwintering and crop-based supplemental resources was essentially the same for our sensitivity test and for our baseline pest population parameters for aphid-type and lygus-type pests (Fig. S6 A and B), and only slightly different

for the whitefly-type pest (Fig. S6C). The direction of the difference in pest load at higher peak densities of the whitefly-type pest tends to amplify, rather than attenuate, the patterns we discuss in the main text. We conclude that, although our simulated pest densities were lower than can be seen in the field during pest outbreaks, our primary results and conclusions are robust with respect to the pest densities reached in our *in silico* experiments.

Fig. S1.

A) Simulated sampling transects for varying values of *k*

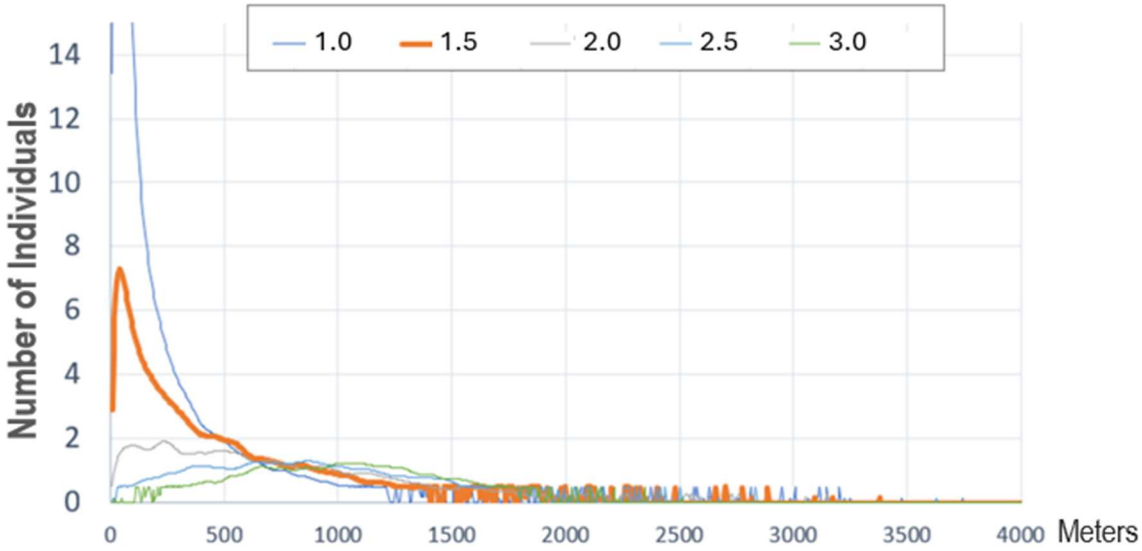

B) *Lygus* recaptures with distance from source

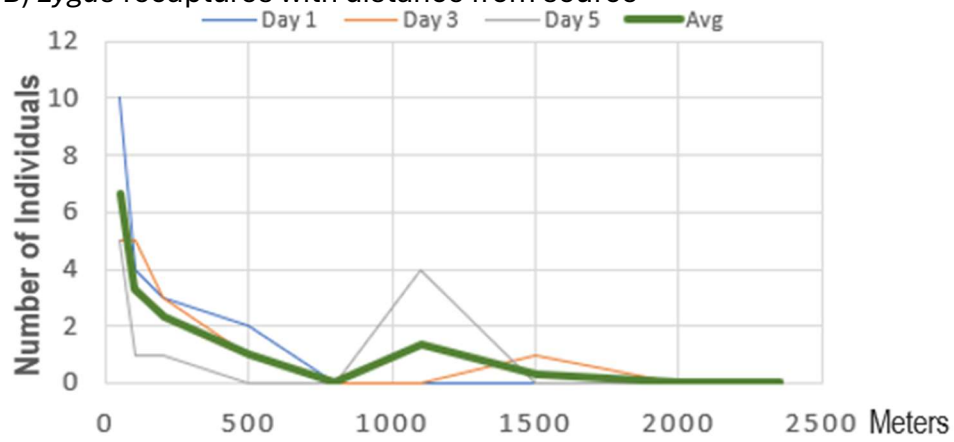

C) *Geocoris* recaptures with distance from source

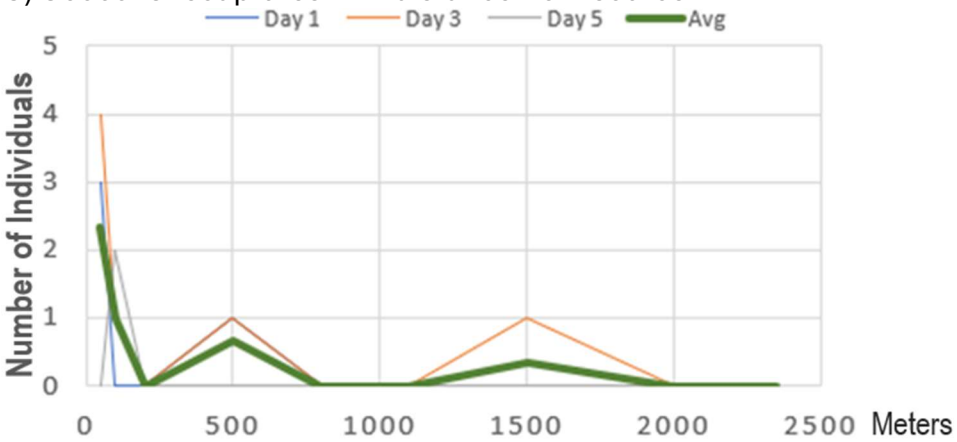

Simulated recaptures (A) versus actual recaptures for Lygus (B) and Geocoris (C) from Sivakoff et al. (S8).

Fig. S2.

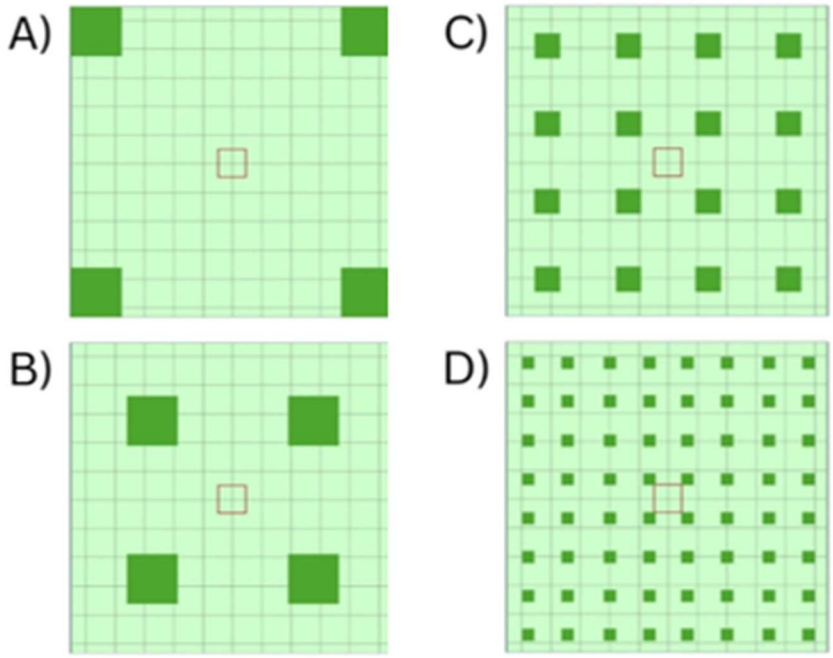

Schematics of configuration of natural habitat in the landscape at 5% total NH coverage for: (A) four NH patches at corners, 8km from center of landscape (note that, because boundaries are reflective, these represent 4 large NH patches centered on the corners of the landscape tile); (B) one patch in each landscape quadrant, each 4km from center of landscape; (C) four patches in each quadrant, closest patch 2 km from center of landscape; (D) 16 patches in each quadrant, closest patch 1 km from center of landscape.

Fig. S3.

A)

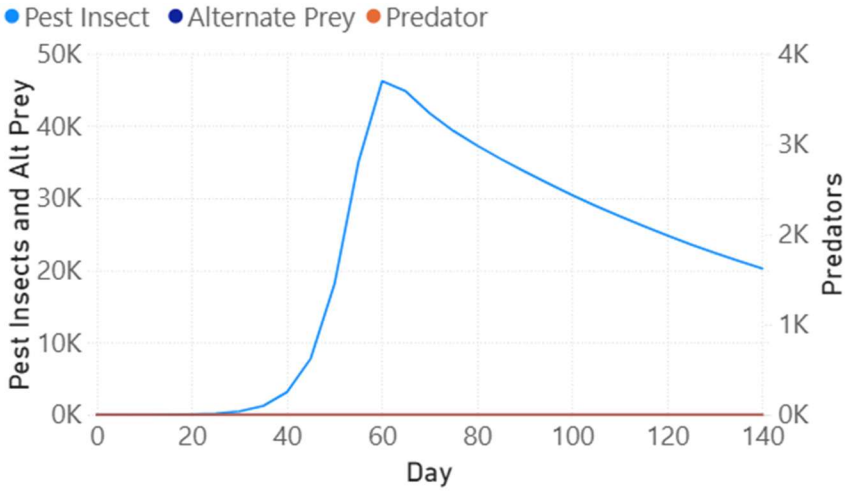

B)

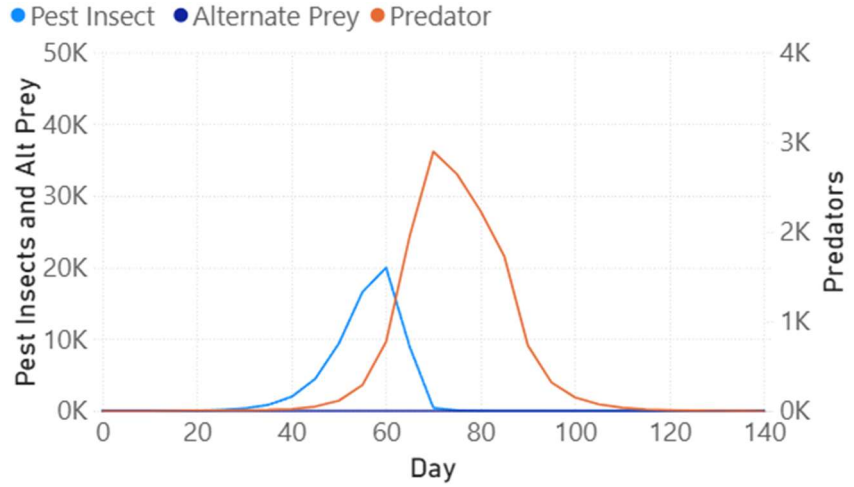

C)

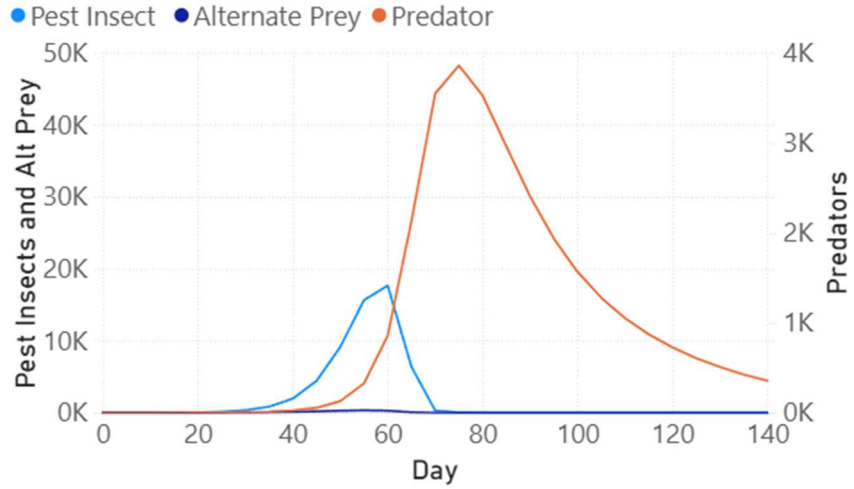

Numbers of aphid-type pest insects, alternate prey, and predators per 100 m^2 for no-predator control (A), overwintering predators but no crop-based resources (B), predators with crop-based resources (C). All runs are with baseline parameters listed in Table S6.

Fig. S4.

A)

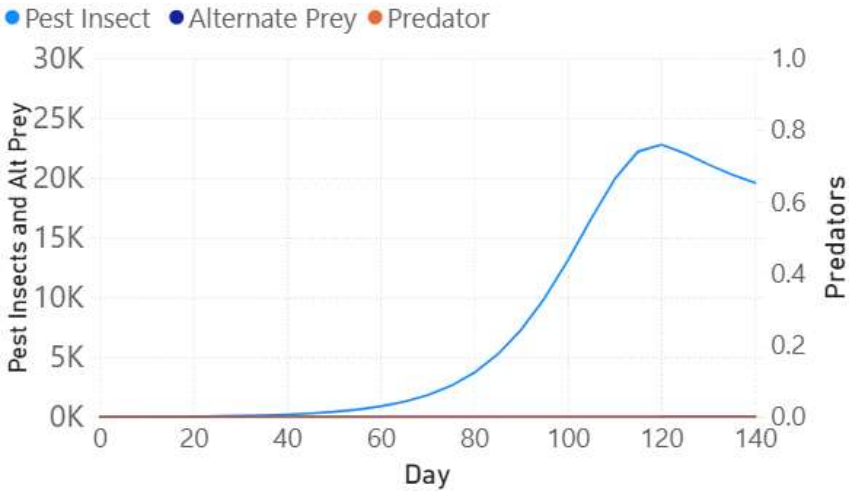

B)

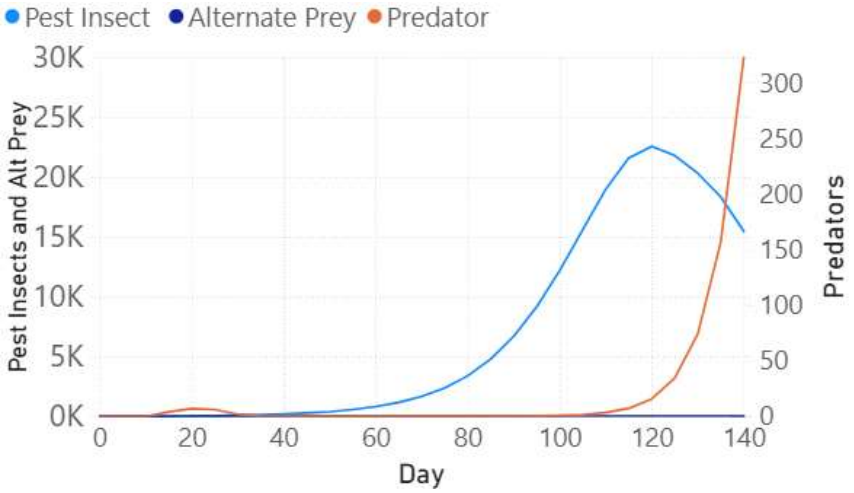

C)

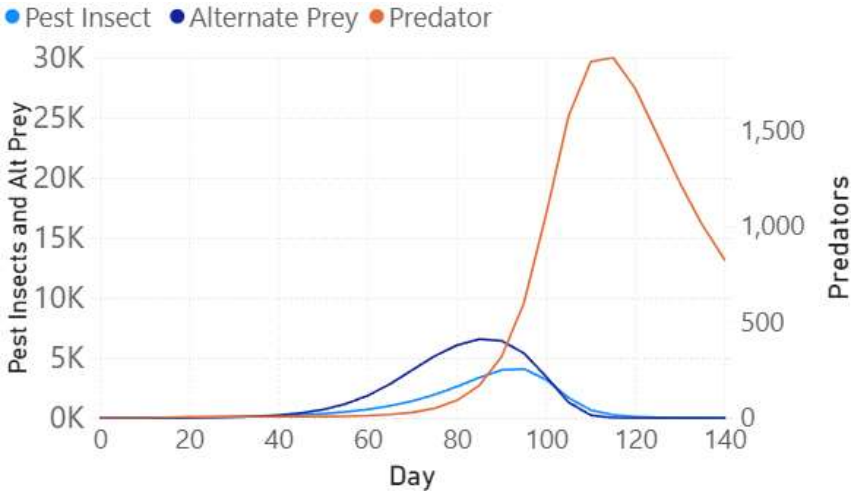

Numbers of lygus-type pest insects, alternate prey, and predators per 100 m^2 for no-predator control (A), overwintering predators but no crop-based resources (B), predators with crop-based resources (C). All runs are with baseline parameters listed in Table S6.

Fig. S5.

A)

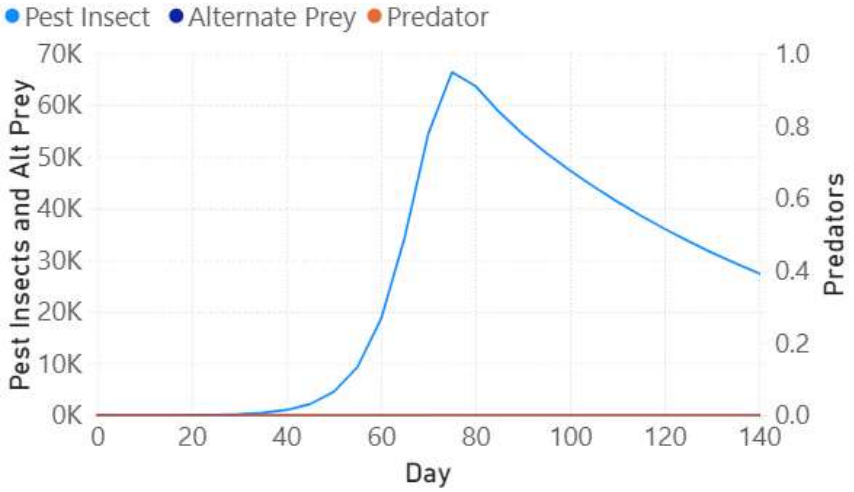

B)

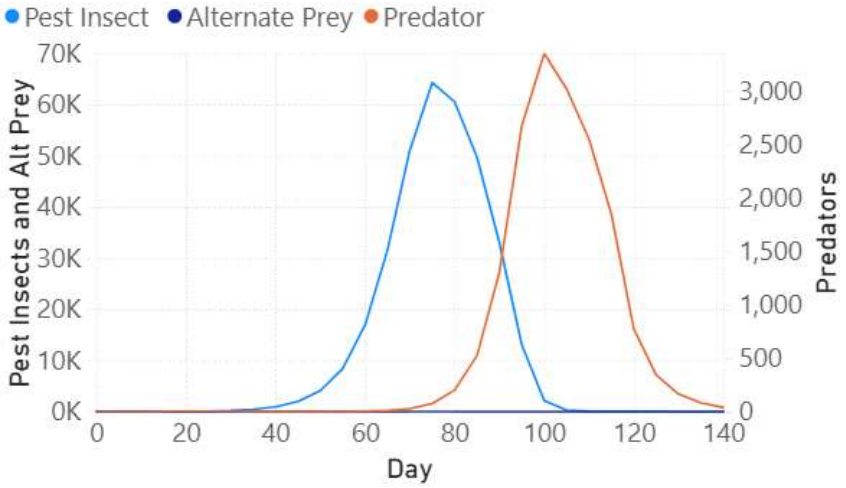

C)

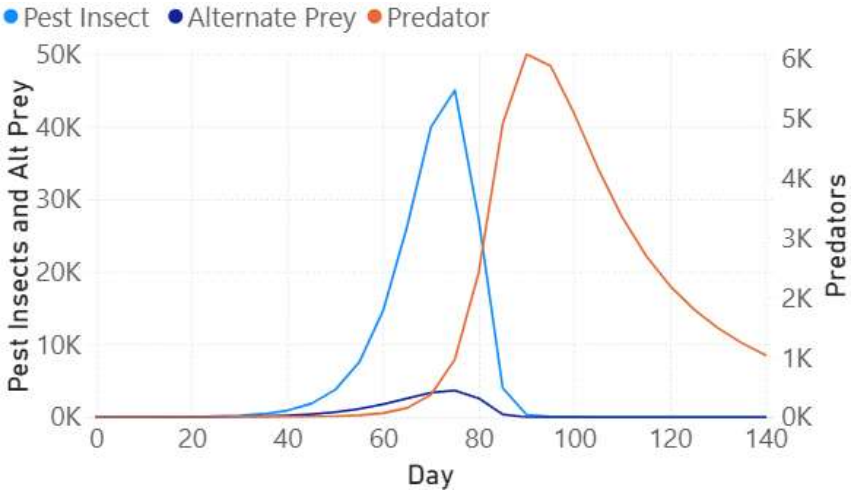

Numbers of whitefly-type pest insects, alternate prey, and predators per 100 m^2 for no-predator control (A), overwintering predators but no crop-based resources (B), predators with crop-based resources (C). All runs are with baseline parameters listed in Table S6.

Fig. S6.

A)

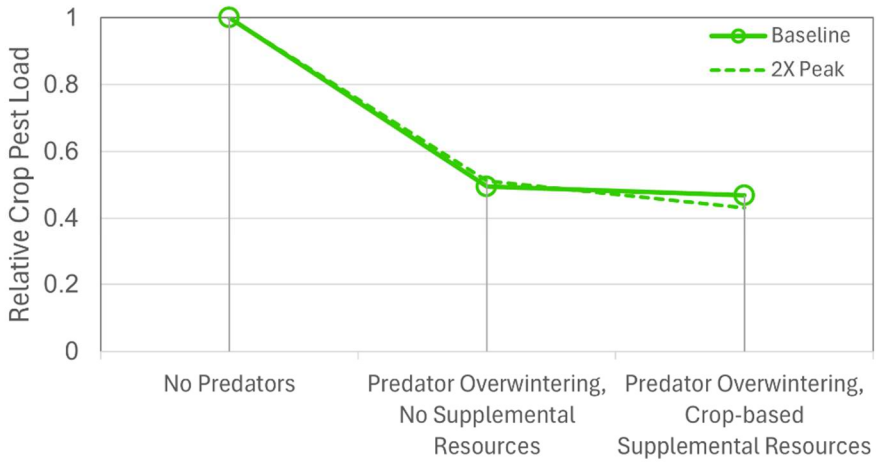

B)

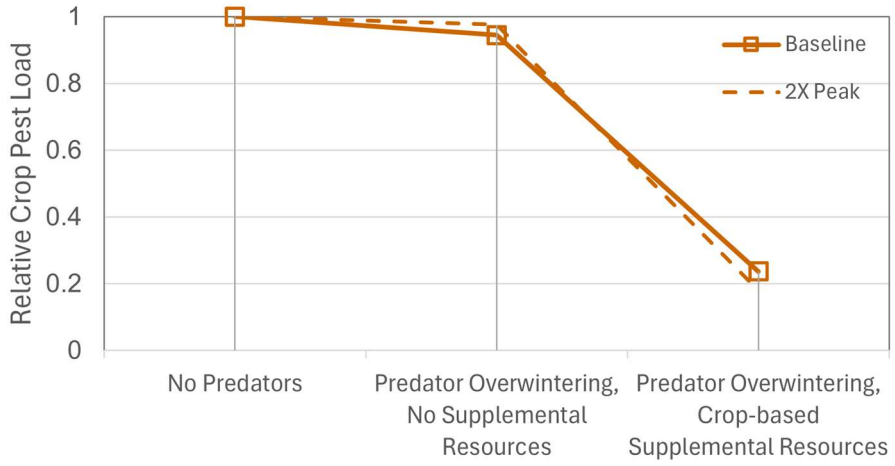

C)

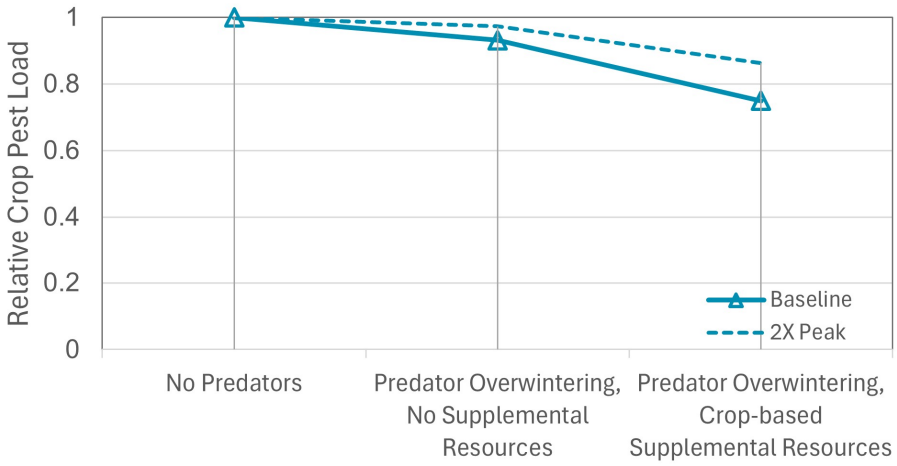

Relative crop pest load with baseline population parameters (solid lines) and with peak populations increased two-fold (dashed lines) for aphid-type (A), lygus-type (B), and whitefly-type (C) pests.

Table S1.

Pest Insect Parameters. *NOTE*: For parameters that vary between pest population types, values are shown separately for lygus-, aphid-, and whitefly-types. Support/Rationale apply to Lygus spp. Parameter values for aphid- and whitefly-types are adjusted relative to lygus value to achieve the desired pest population type attributes (see main text). Symbols match variables in Mathematical Model and Implementation.

Parameter		*Symbol*	*Value*	*Interpretation*	*Support/Rationale*
Population Growth	Egg hatch rate	*ej*	lygus: 0.087/day aphid: 0.173/day whitefly: 0.173/day	Median duration: lygus: 8 days aphid: 4 days whitefly: 4 days	Ugine (S9)
	Nymph maturation rate	*ja*	lygus: 0.033/day aphid: 0.069/day whitefly: 0.069/day	Median duration: lygus: 21 days aphid: 10 days whitefly: 10 days	Ugine (S9)
	External mortality rate	d_i	0.0866/day	Rate of loss of eggs and nymphs to external mortality sources *other than predation*	Fleischer & Gaylor (S10)
	Adult minimum (intrinsic) mortality rate	d_o	0.0495/day	Median longevity: 14 days (under ideal conditions)	Ugine (S9)
	Max fecundity	b_o	lygus: 4 eggs/day aphid: 6 eggs/day whitefly: 4 eggs/day	Fecundity when cumulative density is low	Ugine (S9)
Density Dependence	Adult maximum mortality	d_{max}	lygus: 0.099/day aphid: 0.1386/day	Median longevity above critical threshold:	*Speculative* Assumes slightly higher mortality for aphid and

			whitefly: 0.1386/day	lygus: 7 days aphid: 5 days whitefly: 5 days	whitefly types at peak densities.
	Min fecundity	b_{min}	lygus: 1.25 eggs/d aphid: 0.80 eggs/d whitefly: 0.75 eggs/d	Fecundity when cumulative density is above critical threshold.	*Speculative* Assumes slightly lower fecundity for aphid and whitefly types at peak densities.
	Critical cumulative density	C_{crit}	lygus: 0.25 aphid: 0.50 whitefly: 0.30 Units: (/cm^2) x days	At critical cumulative density mortality is at maximum and fecundity is at minimum.	Populations approach treatment thresholds at peak. See Table 1 in main text.
	Proportion of leaf surface occupied by pest population	Θ_L	lygus: 1.00 aphid: 0.33 whitefly: 1.00	Degree of aggregation of pest population. Note that foraging predators are assumed to restrict their search to the area occupied by the respective pest population.	Lygus is highly mobile. Whitefly tend to disperse across the leaf surface. Aphids generally occur in distinct colonies.
Movement	Minimum diffusion rate	$D_{N_{min}}$	50 m^2/day	Comparable to field measurements of lygus diffusion & other plant bugs.	Fleischer et al. (S11) Bancroft (S12)
	Maximum diffusion rate	$D_{N_{max}}$	200 m^2/day	Comparable to field measurements of lygus diffusion & other plant bugs.	Fleischer et al. (S11) Bancroft (S12)
	Proportional reflection at host/non-host boundaries	ρ	0.8	80% of diffusing pest insects return to the original location on encountering a host -> non-host boundary	*Speculative*

	Dispersal distance parameter	λ	1600	Distance parameter for the Weibull distribution. Median flight distance.	See *Rationale for Weibull distribution parameters*
	Dispersal shape parameter	k	1.5	Shape parameter for the Weibull distribution. Results in classic Weibull fat-tail distribution.	See *Rationale for Weibull distribution parameters*
	Proportional dispersal rate relative to mortality	ψ_{Pest}	1.0	An equal number of adult pests disperse as would die at time t.	*Speculative*
Overwintering	Number of pest insects overwintering	$N_{O_{t=0}}$	8/m^2	Adult pest insects overwinter in *field margins only* at a density of 8/m^2	Fye (S7) Horton & Lewis (S5) See *Rationale for the parameter value for overwintering densities of pest insects and predators*
	Rate of emergence from overwintering	$erate_{No}$	0.693/day	Median time to emergence: 1 day	*Speculative*
	Day emergence from overwintering commences	T_{No}	Day 14	Pest insects start emerging from overwintering roughly 2 weeks after crop germination	*Speculative*
	Proportion dispersing at emergence	$pDisp_{No}$	0.5	50% of emerging predators immediately disperse.	*Speculative*

Table S2.

Predator Parameters

Parameter		*Symbol*	*Value*	*Interpretation*	*Support/Rationale*
Population Growth	Egg hatch rate	ej_P	0.1386/day	Median duration: 5 days	*Speculative*. Set to half of nymph stage duration.

	Nymph maturation rate	ja_P	0.0462/day	Median duration: 15 days	Torres et al. (S13)
	Minimum (intrinsic) mortality rate	pd_{min}	0.0347/day	Median longevity: 20 days	Torres et al. (S13)
	Maximum mortality	pd_{max}	0.345/day	Median longevity: 2 days (following exhaustion of sugar reserves)	*Speculative*
Predation Rate	Max predation rate	Hol_K	20 prey/day	Maximum prey consumed per day. K parameter for Holling Type II functional response	Torres et al. (S13)
	Rate of approach to max predation	Hol_D	25	Prey availability at which consumption is ½ K. D parameter for Holling Type II functional response	*Speculative*
	Predator Search area	pr_{search}	2000 cm^2/ day	Multiplying by prey density gives number of prey currently available to predator, which is then used in Holling Type II function.	Naranjo & Hagler (S14)
	Relative predation by nymphs	j_{pr}	0.25	Nymphs follow the same functional response but are assumed to have a predation rate 25% that of adults.	Torres et al. (S13)
	Predation rate at which nymph mortality starts to rise	pj_{min}	1 prey/day	When nymphs are consuming less than 1 prey/day, mortality increases linearly to max.	*Speculative*
Egg Reserve & Oviposition	Energy value of prey	u	1.33 units	Each prey provides 1.33 total units of nutrition to the predator. A proportion is routed to the egg reserve; the rest to the sugar reserve.	Nutrition units are in the number of eggs produced from consuming the units. For simplicity, sugar units are equated to egg units; the meaning of sugar units should be interpreted as relative to the daily

					maintenance energy cost.
	Proportion of prey energy to eggs	pn_C	0.75	75% of prey energy goes to the egg reserve. Given u=1.33, one egg is produced for every prey item consumed. The remainder (25%) goes to sugar reserves.	Morales-Ramos et al (S15) Finke (S16) (Carbohydrates are low proportion of macronutrient content of insects)
	Oviposition rate	o	0.25/day	Median time from prey consumption to oviposition: 2.77 days. (Note that the egg reserve is in "egg equivalents").	Bueno et al. (S17) (Comparable to pre-oviposition period at 25 deg C)
Sugar Reserve & Daily Maintenance	Daily maintenance cost	m	0.2 units	Each predator uses 0.2 units from the sugar reserve each day for maintenance.	--
	Initial sugar reserve	s_{init}	2.0 units	10 days of maintenance energy	*Speculative*.
	Amount of sugar in reserve at which mortality starts to increase	s_{min}	0.4 units	2 days of maintenance energy	*Speculative*
	Consumption rate	flr_{max}	50 days/day	When floral resources are available, predators can consume them at a rate of 50 days' worth of energy in a day. (But see *Max sugar reserve* below).	See *Rationale for parameter value for the energy consumed per day by a predatory bug feeding on floral resources*
	Predation rate at switch to floral resources	pr_{crit}	10/day	Predators start making use of floral resources when the predation rate falls below 10 prey/day. Floral consumption rate increases proportionally, and linearly as predation rate	*Speculative* Limburg & Rosenheim (S18) report a similar prey-dependent switch by larval lacewings.

				declines from 10 to 0 prey/day.	
	Max sugar reserve	s_{max}	10 days	Predators can hold no more than 10 days' worth of energy in reserve.	*Speculative*. We assume a limit to the amount of sugar energy a predator can hold in reserve at any one time.
Movement	Minimum diffusion rate	$D_{P_{min}}$	25 m^2/day	On average, it is comparable to herbivore diffusion. Stronger response to changing resource conditions.	See herbivore
	Maximum diffusion rate	$D_{P_{max}}$	400 m^2/day	On average, it is comparable to herbivore diffusion. Stronger response to changing resource conditions.	See herbivore
	Dispersal rate relative to mortality	ψ_{Pred}	1.0	The proportion of adults dispersing per day is tied to mortality rate.	*Speculative*
	Dispersal distance parameter	λ	1600	This is the distance parameter for the Weibull distribution. Median flight distance.	See *Rationale for Weibull distribution parameters*
	Dispersal shape parameter	k	1.5	This is the shape parameter for the Weibull distribution. Results in classic Weibull fat-tail distribution.	See *Rationale for Weibull distribution parameters*
Overwintering	Number overwintering	$P_{O_{t=0}}$	4/m^2	Adult predators overwinter in *natural habitat only* at a density of 4/m^2. One half the density of overwintering pest insects.	Fye (S7) Horton & Lewis (S5) See *Rationale for the parameter value for overwintering densities of pest insects and predators*
	Overwintering pred initial sugar reserve	s_{rsv}	2 units	10 days' worth.	*Speculative*
	Rate of emergence	$erate_{Po}$	0.693/day	Median time to emergence: 1 day	*Speculative*

	from overwintering				
	Day emergence from overwintering commences	T_{Po}	Day 14	Predators start emerging from overwintering roughly 2 weeks after crop germination. Same day as pest insect.	*Speculative*
	Proportion dispersing at emergence	$pDisp_{Po}$	0.5	50% of emerging predators immediately disperse.	*Speculative*

Table S3.

Alternate Prey Parameters

Parameter		*Symbol*	*Value*	*Interpretation*	*Support/Rationale*
Population Growth	Carrying capacity in crop	K_D	0.004/cm^2	Logistic growth used for alt prey. K is per unit leaf area. Equivalent to 0.4 alt prey every 100cm^2 of leaf surface.	Results in maximum number of alternate prey roughly half of peak numbers of pest insect without predation.
	Growth rate	r	0.12/day	r in logistic growth equation	Alternate prey reach carrying capacity half-way through season.
Movement	Diffusion Rate when cell supports alternate prey	D_H	100 m^2/day	Comparable to pest insect and predator at average conditions.	--
	Proportional reflection at host/non-host boundaries	ρ	0.8	80% of diffusing alternate prey return to the original location on encountering a host -> non-host boundary	*Speculative*
	Dispersal distance parameter	λ	1600	Distance parameter for the Weibull distribution. Same as pest insect.	See *Rationale for Weibull distribution parameters*
	Dispersal shape parameter	k	1.5	Shape parameter for the Weibull distribution. Same as pest insect.	See *Rationale for Weibull distribution parameters*
	Dispersal rate relative to mortality	$\psi_{Alt\text{-}prey}$	0.05	Alternate prey disperse at a 5% rate if density is greater than K_D /2	*Speculative*

Overwintering	Number overwintering	$H_{O_{t=0}}$	8/m^2	Alternate prey overwinter in *field margins only* at a density of 8/m^2. Same density as pest insect.	Fye (S7) Horton & Lewis (S5) See *Rationale for the parameter value for overwintering densities of pest insects and predators*
	Rate of emergence from overwintering	$erate_{Ho}$	0.693/day	Median time to emergence: 1 day	*Speculative*
	Day emergence from overwintering commences	T_{Ho}	Day 14	Alternate prey start emerging from overwintering roughly 2 weeks after crop germination. Same day as pest insect.	*Speculative*
	Proportion dispersing at emergence	$pDisp_{Ho}$	0.5	50% of emerging alternate prey immediately disperse.	*Speculative*

Table S4.

Vegetation parameters

Parameter		*Symbol*	*Value*	*Interpretation*	*Support/Rationale*
Crop	Max LAI	α	3.0	Maximum leaf area index. Comparable to cotton.	Ko et al. (S19) Other estimates of cotton LAI in literature are both lower and higher than ~3.
	Growth rate	β	0.025/day	Rate at which LAI approaches max. LAI is 90% of max halfway through the season.	Ko et al. (S19)
	Initial Days of Growth	T_{init}	2	Two days of growth at initialization	--
	Floral resources	*flr*	True/False	Presence of floral resources in the crop varies by scenario	
	Host Status: Pest	--	Yes	Crop is host plant for the pest insect. All parameters as in table above.	
	Host Status: Alt Prey	--	Yes/No	Whether the crop supports an alternate prey population varies by	Assumes minimal density and high rate of trivial movement on non-host.

				scenario. If not a host, alternate prey parameters become: • K_D = 0.00001 / cm^2 • D_H = 200 m^2/day	
Natural Habitat Vegetation	Max LAI	α	5.0	Maximum LAI for semi-natural habitat	*Speculative*. Actual max LAI will vary greatly depending on the make-up of the natural habitat. Asner et al. (S20)
	Initial Days of Growth	T_{init}	30	30 days of growth at initialization	*Speculative*. Assume some growth of natural habitat vegetation has occurred prior to crop planting.
	Growth rate	β	0.01	Rate at which LAI approaches max.	*Speculative*. Assume growth rate roughly half that of a managed agricultural crop.
	Floral resources	*flr*	False	There are no floral resources in the natural habitat.	
	Host Status: Pest	--	No	Natural habitat is not a host plant for the pest insect. Parameters become: • C_{crit} = 0 (/cm^2) x days • b_{max} = 0 eggs/day • d_{min} = 0.1386/day • D_{min} = 200 m^2/day	Assumes no egg laying, high morality, and high trivial movement in non-host vegetation.
	Host Status: Alt Prey	--	No	Natural habitat is not a host for alternate prey, parameters become: • K_D = 0.00001 / cm^2 • D_H = 200 m^2/day	Assumes minimal density and high rate of trivial movement on non-host.

Field Margins Vegetation	Max LAI	α	1.5	Maximum LAI for field margins	*Speculative*. Actual max LAI will vary greatly depending on the make-up of the natural habitat. Asner et al. (S20)
	Initial Days of Growth	T_{init}	15	15 days of growth at initialization.	*Speculative*. Assume some growth of field margin vegetation has occurred prior to crop planting.
	Growth rate	β	0.01	Rate at which LAI approaches max.	*Speculative*. Assume growth rate roughly half that of a managed agricultural crop.
	Floral resources	*flr*	False	There are no floral resources in field margins.	
	Host Status: Pest	--	No	Field margins are not a host plant for the pest insect. Parameters become: • C_{crit} = 0 (/cm^2) x days • b_{max} = 0 eggs/day • d_{min} = 0.1386/day • D_{min} = 200 m^2/day	Assumes no egg laying, high morality, and high movement in non-host vegetation.
	Host Status: Alt Prey	--	No	Field margins are not a host for alternate prey, parameters become: • K_D = 0.00001 / cm^2 • D_H = 200 m2/day	Assumes minimal density and high rate of movement on non-host.

Table S5.

Parameters and peak density for three simulated pest population types

Pest Population Type	Egg+ Nymph Duration	Max Oviposition Rate	% Leaf Area Occupied	Peak Density per Leaf (100 cm^2/ leaf)
Aphid-type	14 days	6/day	33%	5.9/leaf

Lygus-type	29 days	4/day	100%	0.8/leaf
Whitefly-type	14 days	4/day	100%	2.6/leaf

Table S6.

Parameters used in simulation experiments. Only one experimental variable is manipulated at a time; other variables retain their baseline values, indicated in bold.

Experimental Variable	**Parameter values**				
%NH	1.25%	2.5%	**5%**	10%	20%
NH Distribution (distance from center of landscape to nearest NH patch)		1 km	**2 km**	4 km	8 km
Predator overwintering density	$1/m^2$	$2/m^2$	**$4/m^2$**	$8/m^2$	$16/m^2$
Median dispersal distance	400 m	800 m	**1600 m**	3200 m	6400 m
% Dispersal at emergence	0%	25%	**50%**	75%	100%
Day of emergence		Day 0	**Day 14**	Day 28	Day 42
Energy reserve at emergence	1 day	5 days	**10 days**	20 days	

Table S7.

Full linear model output for predator immigration rate versus experimental variables.

	Estimate	Standardized	Std. Error	t value	Pr(>|t|)	
(Intercept)	9.615e-03	NA	3.524e-02	0.273	0.7853	
NHDist	-6.123e-02	-1.740e-01	1.176e-02	-5.205	6.61e-07	***
PercentNH	7.373e-02	5.433e-01	4.532e-03	16.270	< 2e-16	***
CropResYes	-7.192e-02	-8.331e-02	4.983e-02	-1.443	0.1511	
DispersalDist	5.135e-05	1.211e-01	1.416e-05	3.626	0.0004	***
PctDispersal	5.247e-01	1.885e-01	9.278e-02	5.655	8.20e-08	***
PredDens	1.120e-01	6.601e-01	5.665e-03	19.764	< 2e-16	***
PredEmergence	-3.717e-03	-5.717e-02	2.171e-03	-1.712	0.0890	.
SugarReserve	-1.004e-02	-6.539e-02	5.120e-03	-1.962	0.0518	.
PestTypeL	1.058e-01	1.155e-01	4.983e-02	2.122	0.0355	*
PestTypeW	7.346e-02	8.023e-02	4.983e-02	1.474	0.1426	
CropResYes:PestTypeL	-1.115e-01	-9.630e-02	7.048e-02	-1.583	0.1157	
CropResYes:PestTypeW	-8.885e-02	-7.671e-02	7.048e-02	-1.261	0.2095	

Signif. codes: 0 ‘***’ 0.001 ‘**’ 0.01 ‘*’ 0.05 ‘.’ 0.1 ‘ ’ 1

Residual standard error: 0.1797 on 143 degrees of freedom
Multiple R-squared: 0.8412, Adjusted R-squared: 0.8278
F-statistic: 63.11 on 12 and 143 DF, p-value: < 2.2e-16

Parameter	Eta2 (partial)	95% CI
NHDist	0.24	[0.14, 1.00]
PercentNH	0.63	[0.56, 1.00]
CropRes	0.14	[0.06, 1.00]
DispersalDist	0.06	[0.01, 1.00]
PctDispersal	0.18	[0.10, 1.00]
PredDens	0.73	[0.68, 1.00]
PredEmergence	0.02	[0.00, 1.00]
SugarReserve	0.03	[0.00, 1.00]
PestType	0.01	[0.00, 1.00]
CropRes:PestType	0.02	[0.00, 1.00]

- One-sided CIs: upper bound fixed at [1.00].

Legend:

NHDist=Distribution of NH; CropResYes=Supplemental resources present in crop vs absent; DispersalDist=Median Dispersal Distance; PctDispersal=Percent of predators dispersing on emergence; PredDens=Density of overwintering predators in NH; PredEmergence=Day of emergence; PestTypeL=Lygus-type vs Aphid-type; PestTypeW=Whitefly-type vs Aphid-type

Table S8.

Full linear model output for predator energy accumulation versus experimental variables.

	Estimate	Standardized	Std. Error	t value	Pr(>|t|)	
(Intercept)	1.186e-02	NA	1.993e-01	0.060	0.95263	
NHDist	-1.449e-02	-5.172e-03	6.655e-02	-0.218	0.82797	
PercentNH	-7.425e-03	-6.873e-03	2.564e-02	-0.290	0.77254	
CropResYes	2.619e+00	3.811e-01	2.819e-01	9.289	2.35e-16	***
DispersalDist	-4.467e-05	-1.323e-02	8.012e-05	-0.558	0.57799	
PctDispersal	1.517e+00	6.846e-02	5.249e-01	2.891	0.00445	**
PredDens	-1.202e-02	-8.899e-03	3.205e-02	-0.375	0.70824	
PredEmergence	-1.227e-01	-2.370e-01	1.228e-02	-9.988	< 2e-16	***
SugarReserve	1.683e-01	1.377e-01	2.896e-02	5.811	3.87e-08	***
PestTypeL	-5.525e+00	-7.581e-01	2.819e-01	-19.599	< 2e-16	***
PestTypeW	-2.660e+00	-3.649e-01	2.819e-01	-9.434	< 2e-16	***
CropResYes:PestTypeL	5.665e+00	6.145e-01	3.987e-01	14.210	< 2e-16	***
CropResYes:PestTypeW	2.778e+00	3.013e-01	3.987e-01	6.967	1.09e-10	***

Signif. codes: 0 ‘***’ 0.001 ‘**’ 0.01 ‘*’ 0.05 ‘.’ 0.1 ‘ ’ 1

Residual standard error: 1.016 on 143 degrees of freedom
Multiple R-squared: 0.9198, Adjusted R-squared: 0.913
F-statistic: 136.6 on 12 and 143 DF, p-value: < 2.2e-16

Parameter	Eta2 (partial)	95% CI
NHDist	4.46e-04	[0.00, 1.00]
PercentNH	4.01e-05	[0.00, 1.00]
CropRes	0.89	[0.86, 1.00]
DispersalDist	2.75e-04	[0.00, 1.00]
PctDispersal	0.06	[0.01, 1.00]
PredDens	1.79e-06	[0.00, 1.00]
PredEmergence	0.41	[0.31, 1.00]
SugarReserve	0.19	[0.10, 1.00]
PestType	0.56	[0.47, 1.00]
CropRes:PestType	0.59	[0.50, 1.00]

- One-sided CIs: upper bound fixed at [1.00].

Legend:

NHDist=Distribution of NH; CropResYes=Supplemental resources present in crop vs absent; DispersalDist=Median Dispersal Distance; PctDispersal=Percent of predators dispersing on emergence; PredDens=Density of overwintering predators in NH; PredEmergence=Day of emergence; PestTypeL=Lygus-type vs Aphid-type; PestTypeW=Whitefly-type vs Aphid-type

Table S9.

Full linear model output for aphid-type pest load versus predator population metrics.

	Estimate	Standardized	Std. Error	t value	Pr(>|t|)
(Intercept)	0.387270	NA	0.008883	43.599	< 2e-16 ***
Immigration	-0.335188	-0.885852	0.024702	-13.570	< 2e-16 ***
Sugar	-0.023468	-0.326003	0.004604	-5.097	5.79e-06 ***
Immigration:Sugar	-0.039965	-0.199790	0.013250	-3.016	0.00409 **

Signif. codes: 0 ‘***’ 0.001 ‘**’ 0.01 ‘*’ 0.05 ‘.’ 0.1 ‘ ’ 1

Residual standard error: 0.06405 on 48 degrees of freedom
Multiple R-squared: 0.81, Adjusted R-squared: 0.7981
F-statistic: 68.2 on 3 and 48 DF, p-value: < 2.2e-16

Parameter	Eta2 (partial)	95% CI
Immigration	0.78	[0.69, 1.00]
Sugar	0.31	[0.14, 1.00]
Immigration:Sugar	0.16	[0.03, 1.00]

- One-sided CIs: upper bound fixed at [1.00].

Legend:

Immigration=Immigrating predators per cell per day; Sugar=Average days’ worth of energy per predator

Table S10.

Full linear model output for lygus-type pest load versus predator population metrics.

	Estimate	Standardized	Std. Error	t value	Pr(>|t|)
(Intercept)	0.133499	NA	0.004820	27.697	< 2e-16 ***
Immigration	-0.039745	-0.258352	0.011914	-3.336	0.00165 **
Sugar	-0.014726	-0.897353	0.001110	-13.262	< 2e-16 ***
Immigration:Sugar	-0.008695	-0.234526	0.002836	-3.066	0.00356 **

Signif. codes: 0 ‘***’ 0.001 ‘**’ 0.01 ‘*’ 0.05 ‘.’ 0.1 ‘ ’ 1

Residual standard error: 0.03415 on 48 degrees of freedom
Multiple R-squared: 0.7881, Adjusted R-squared: 0.7749
F-statistic: 59.52 on 3 and 48 DF, p-value: 3.351e-16

Parameter	Eta2 (partial)	95% CI
Immigration	5.96e-05	[0.00, 1.00]
Sugar	0.78	[0.69, 1.00]
Immigration:Sugar	0.16	[0.04, 1.00]

- One-sided CIs: upper bound fixed at [1.00].

Legend:
Immigration=Immigrating predators per cell per day; Sugar=Average days' worth of energy per predator

Table S11.

Full linear model output for whitefly-type pest load versus predator population metrics.

	Estimate	Standardized	Std. Error	t value	Pr(>|t|)
(Intercept)	0.2770447	NA	0.0019156	144.63	< 2e-16 ***
Immigration	-0.0789837	-0.8945637	0.0050489	-15.64	< 2e-16 ***
Sugar	-0.0090000	-0.6801405	0.0006385	-14.10	< 2e-16 ***
Immigration:Sugar	-0.0213954	-0.6935242	0.0017526	-12.21	2.5e-16 ***

Signif. codes: 0 '***' 0.001 '**' 0.01 '*' 0.05 '.' 0.1 ' ' 1

Residual standard error: 0.01366 on 48 degrees of freedom
Multiple R-squared: 0.8916, Adjusted R-squared: 0.8848
F-statistic: 131.6 on 3 and 48 DF, p-value: < 2.2e-16

Parameter	Eta2 (partial)	95% CI
Immigration	0.64	[0.50, 1.00]
Sugar	0.77	[0.67, 1.00]
Immigration:Sugar	0.76	[0.65, 1.00]

- One-sided CIs: upper bound fixed at [1.00].

Legend:
Immigration=Immigrating predators per cell per day; Sugar=Average days' worth of energy per predator

References.

1. May, P. G. (1988). Determinants of foraging profitability in two nectarivorous butterflies. Ecological Entomology, 13(2), 171-184.

2. Cardoso, M.Z. and Gilbert, L.E. (2013), Pollen feeding, resource allocation and the evolution of chemical defense in passion vine butterflies. J. Evol. Biol., 26: 1254-1260.

3. Cohen, A. C., & Staten, R. T. (2018). Long-term culturing and quality assessment of predatory big-eyed bugs, Geocoris punctipes. In Applications of genetics to arthropods of biological control significance (pp. 121-132). CRC Press.

4. Cohen, A. C., & Byrne, D. N. (1992). Geocoris punctipes as a predator of Bemisia tabaci: a laboratory evaluation. Entomologia Experimentalis et Applicata, 64(2), 195-202.

5. Horton, D. R., & Lewis, T. M. (2003). Numbers and types of arthropods overwintering on common mullein, Verbascum thapsus L.(Scrophulariaceae), in a central Washington fruit-growing region. Journal of the Entomological Society of British Columbia, 100, 79-87.

6. Reinartz, J. A. (1984). Life history variation of common mullein (Verbascum thapsus): I. Latitudinal differences in population dynamics and timing of reproduction. The Journal of Ecology, 897-912.

7. Fye, R. E. (1975). Plant host sequence of major cotton insects in southern Arizona (Vol. 24). US Department of Agriculture, Agricultural Research Service, Western Region.

8. Sivakoff, F. S., Rosenheim, J. A., & Hagler, J. R. (2012). Relative dispersal ability of a key agricultural pest and its predators in an annual agroecosystem. Biological Control, 63(3), 296-303.

9. Ugine TA. Developmental times and age-specific life tables for *Lygus lineolaris* (Heteroptera: Miridae), reared at multiple constant temperatures. Environ Entomol. 2012 Feb;41(1):1-10.

10. S. J. Fleischer AND M. J. Gaylor. 1988. *Lygus lineolaris* (Heteroptera: Miridae) Population Dynamics: Nymphal Development, Life Tables, and Leslie Matrices on Selected Weeds and Cotton. Environ. Entomol. 17(2): 246-253

11. Fleischer, S. J., Gaylor, M. J., & Hue, N. V. (1988). Dispersal of *Lygus lineolaris* (Heteroptera: Miridae) adults through cotton following nursery host destruction. Environmental entomology, 17(3), 533-541.

12. Bancroft, J. S. (2005). Dispersal and abundance of *Lygus hesperus* in field crops. Environmental Entomology, 34(6), 1517-1523.

13. J. B. Torres, C. S. A. Silva-Torres, AND J. R. Ruberson. 2001. Effect of Two Prey Types on Life-History Characteristics and Predation Rate of Geocoris floridanus (Heteroptera: Geocoridae). Environ. Entomol. 33(4): 964-974

14. S. E. Naranjo & J. R. Hagler. 2001. Toward the Quantification of Predation with Predator Gut Immunoassays: A New Approach Integrating Functional Response Behavior Biological Control 20, 175–189

15. Juan A. Morales-Ramos, M. Guadalupe Rojas, Thomas A. Coudron, Man P. Huynh, Deyu Zou, Kent S. Shelby, Chapter 8 - Artificial diet development for entomophagous arthropods, Editor(s): Juan A. Morales-Ramos, M. Guadalupe Rojas, David I. Shapiro-Ilan, Mass Production of Beneficial Organisms (Second Edition), Academic Press, 2023, Pages 233-260

16. Finke, M.D. (2002), Complete nutrient composition of commercially raised invertebrates used as food for insectivores. Zoo Biol., 21: 269-285.

17. V. H. P. Bueno, A. M. Calixto, F. C. Montes & J. C. van Lenteren. Reproduction and population parameters of the Nearctic predator *Geocoris punctipes* at constant and varying temperature regimes. J. Appl. Entomol. 140(2016) 323–333

18. Limburg, D. D., and J. A. Rosenheim. 2001. Extrafloral nectar consumption and its influence on the survival and development of an omnivorous predator, larval *Chrysoperla carnea*. Environmental Entomology 30:595-604

19. Ko, J., Maas, S.J., Lascano, R.J. and Wanjura, D. (2005), Modification of the GRAMI Model for Cotton. Agron. J., 97: 1374-1379.

20. Asner, G. P., Scurlock, J. M., & A. Hicke, J. (2003). Global synthesis of leaf area index observations: implications for ecological and remote sensing studies. *Global ecology and biogeography*, *12*(3), 191-205.